Protocol

Visualization of metabolites and microbes at high spatial resolution using MALDI mass spectrometry imaging and in situ fluorescence labeling

Patric Bourceau[1,2,7], Benedikt Geier ⓘ [1,3,7], Vincent Suerdieck[4], Tanja Bien ⓘ [4,5], Jens Soltwisch ⓘ [4], Klaus Dreisewerd[4] & Manuel Liebeke ⓘ [1,6] ✉

Abstract

Label-free molecular imaging techniques such as matrix-assisted laser desorption ionization mass spectrometry imaging (MALDI-MSI) enable the direct and simultaneous mapping of hundreds of different metabolites in thin sections of biological tissues. However, in host–microbe interactions it remains challenging to localize microbes and to assign metabolites to the host versus members of the microbiome. We therefore developed a correlative imaging approach combining MALDI-MSI with fluorescence in situ hybridization (FISH) on the same section to identify and localize microbial cells. Here, we detail metaFISH as a robust and easy method for assigning the spatial distribution of metabolites to microbiome members based on imaging of nucleic acid probes, down to single-cell resolution. We describe the steps required for tissue preparation, on-tissue hybridization, fluorescence microscopy, data integration into a correlative image dataset, matrix application and MSI data acquisition. Using metaFISH, we map hundreds of metabolites and several microbial species to the micrometer scale on a single tissue section. For example, intra- and extracellular bacteria, host cells and their associated metabolites can be localized in animal tissues, revealing their complex metabolic interactions. We explain how we identify low-abundance bacterial infection sites as regions of interest for high-resolution MSI analysis, guiding the user to a trade-off between metabolite signal intensities and fluorescence signals. MetaFISH is suitable for a broad range of users from environmental microbiologists to clinical scientists. The protocol requires ~2 work days.

Key points

- A procedure for spatial metabolomics of host–microbe interactions, including tissue preparation, matrix application, MSI data acquisition, on-tissue hybridization using nucleic acid probes, fluorescence microscopy and data integration into a correlative image dataset.

- MALDI-MSI enables single-cell-level mapping of metabolites by revealing their spatial distribution. Alternatively, laser-capture micro-dissection can be combined with LC–MS, or metaFISH combines spatial metabolomics with FISH.

Key references

Geier, B. et al. *Nat. Microbiol.* **5**, 498–510 (2020): https://doi.org/10.1038/s41564-019-0664-6

Geier, B. et al. *Proc. Natl Acad. Sci. USA* **118**, e2023773118 (2021): https://doi.org/10.1073/pnas.2023773118

Bien, T. et al. *Proc. Natl Acad. Sci. USA* **119**, e2114365119 (2022): https://doi.org/10.1073/pnas.2114365119

Niehaus, M. et al. *Nat. Methods* **16**, 925–931 (2019): https://doi.org/10.1038/s41592-019-0536-2

[1]Max Planck Institute for Marine Microbiology, Bremen, Germany. [2]MARUM – Center for Marine Environmental Sciences, University of Bremen, Bremen, Germany. [3]Stanford University School of Medicine, Stanford, CA, USA. [4]Institute of Hygiene, University of Münster, Münster, Germany. [5]Bruker Daltonics GmbH & Co. KG, Bremen, Germany. [6]Institute of Human Nutrition and Food Sciences, University of Kiel, Kiel, Germany. [7]These authors contributed equally: Patric Bourceau, Benedikt Geier. ✉e-mail: mliebeke@mpi-bremen.de

Protocol

Introduction

Pinpointing individual metabolites at the host–microbe interface remains a key challenge in resolving metabolic interactions in microbial mutualism and pathogenesis. The spatial distribution of metabolites reflects communication, defense and nutritional exchange in host–microbiota interactions, and thus needs to be resolved in relation to the individual cell types of host and microbes within a tissue. However, a reliable approach to probe the metabolic and site-specific phenotypes of microbes in complex tissues was missing. Spatial proteomics and transcriptomics have made it easier to locate proteins and genes in eukaryotic hosts, whereas a dependable method for investigating the metabolic and site-specific phenotypes of microbes in complex tissues has been lacking[1,2]. While transcripts and proteins are directly linked to an organism's genome, no direct connection exists for associated metabolites. Uncovering the sources of metabolic heterogeneity in complex tissues requires a method for accurately connecting metabolites with their producing cells, thereby characterizing their metabolic phenotypes.

Conventionally, metabolites are measured from tissue extracts by untargeted metabolomics using chromatographic methods, then combined with mass spectrometry (MS) or nuclear magnetic resonance spectroscopy[3,4]. Unless microdissection techniques are used, the information on the spatial organization of cells and their specific metabolic fingerprint is lost. In the case of bacterial infections, researchers need a tool to resolve the metabolic heterogeneity between healthy and infected cells, which can vary within micrometers. MS imaging (MSI) techniques can map hundreds of different metabolites from a single tissue section in a highly spatially resolved manner referred to as spatial metabolomics[5,6]. Among the suite of different MS-based imaging techniques are matrix-assisted laser desorption ionization MSI (MALDI–MSI), desorption electrospray ionization, secondary ion MS and laser ablation inductively coupled plasma MS, and their application for biological samples is reviewed elsewhere[7–9]. Here, we focus on MALDI–MSI, which provides a wide window to analyze intact biomolecules, including glycans[10,11] and numerous metabolite classes, e.g., sugars[12,13], lipids[14–16] or co-factors[17].

In recent years, 5 µm resolution (pixel size) became available with commercial hardware (Table 1), which allows MALDI–MSI to confidently differentiate individual eukaryotic cells[14,18–20]. Pixel sizes below 5 µm were achieved with an experimental transmission mode device[21] and an atmospheric pressure MALDI setup with advanced optics[22]. Resolutions of 5–10 µm are sufficient to differentiate between colonized and uncolonized eukaryotic cells but cannot resolve most bacterial cells individually (~1 µm). MALDI–MSI has enabled microbiologists to analyze the metabolites from bacterial colonies on agar plates[23,24] and in biofilms[25], whereas metabolite localization on a cellular level has still been rarely applied[26,27].

Even at the highest spatial resolutions, MALDI–MSI alone is often not enough to reliably assign metabolic fingerprints of cells to the respective microbial taxa, as we lack species and strain-specific metabolite biomarkers. It is essential to know the taxonomic identity of the measured cells in combination with mapping the location of metabolites at cellular resolution. To identify individual cells, labeling approaches range from antibodies and fluorescent protein tags to fluorescence in situ hybridization (FISH) of nucleotide sequences[28,29].

FISH is highly versatile, with the potential to label any selected DNA or RNA sequence with a unique fluorescent signal through in silico-designed probes[30–32]. This process does not rely on cell cultivation or genetic manipulation. Organism-specific probes can be designed based on sequencing data (e.g., 16S rRNA sequence retrieved from a metagenome), if no published probes are available[33]. In particular, 16S rRNA FISH has been used to identify and localize microbiome members in tissues[34–36]. The high resolution of fluorescent microscopy and specificity of FISH probes[37,38], in combination with high-resolution MALDI–MSI, links metabolic fingerprints to individual cells of the microbial community[6,39]. The analysis of microbial metabolites in animal samples using MSI and FISH was demonstrated with different MSI setups and a multitude of samples (e.g., surfaces of cocoons, tissues from marine and terrestrial animals)[6,39,40].

Protocol

Instrument	AP-SMALDI-10, AP-SMALDI-5 AF, TransMIT; AP-SMALDI prototype	timsTOF fleX MALDI-2 with microGRID, Bruker Daltonics	t-MALDI-2 prototype
Availability	Commercial (AP-SMALDI-10, AP-SMALDI-5 AF); experimental	Commercial	Experimental
Minimum pixel size[a]	10 µm (AP-SMALDI-10) 5 µm (AP-SMALDI-5 AF) 1.4 µm (AP-SMALDI, experimental)	5 µm	1.2 µm 0.6 µm with oversampling
Mass resolution (FWHM)	240,000 at m/z 200 (with Q Exactive HF)	60,000 at m/z 200	280,000 at m/z 200 (with Q Exactive Plus)
Acquisition speed (at given mass resolution for m/z 200)	1 pixel s^{-1} (AP-SMALDI-10) 1.9 pixel s^{-1} at 240,000 (AP-SMALDI-5 AF) 10 pixel s^{-1} at 30,000 (AP-SMALDI-5 AF)	Up to 10 pixel s^{-1}	1 pixel s^{-1} at 280,000 3.7 pixel s^{-1} at 70,000
Acquisition time for 1 mm² at 5 µm pixel size (200 × 200 pixels)	AP-SMALDI-5 AF:		
	5.8 h at 240,000	1.1 h	11.1 h at 280,000
	1.1 h at 30,000		3 h at 70,000
Postionization	No	Yes	Yes
Ion mobility	No	Yes	No
Examples MSI	Refs. 22,100	Refs. 10,101	Refs. 14,21
Examples metaFISH	This study and ref. 6	This study	This study

[a]The smallest step size supported is below this value, but oversampling will generally occur below the specified pixel size.

With the advancements in correlative MALDI–MSI and FISH microscopy, researchers have gained insights into the molecular mechanisms of multispecies host–microbe systems[41]. Only with both types of information it is possible to decipher in situ metabolism in pathogenesis or microbial mutualism. This can range from pathogen infections (host and one bacterial pathogen) and low-diversity symbiotic interactions (host and one or several symbionts), to complex microbiomes (host and many microbial species). To enable the scientific community to analyze the spatial metabolism in their host–microbe system, we describe how to combine FISH with MALDI–MSI in this protocol.

Development of the protocol

The combined spatial metabolomics and in situ hybridization of the 16S rRNA protocol, which we termed metaFISH, was originally designed for the investigation of symbioses between invertebrates and their bacterial symbionts[6,40]. In one of these exemplary systems, a marine deep-sea mussel of the genus *Bathymodiolus* harbors intracellular symbionts in specialized epithelial cells. The bacterial symbionts provide the host with energy and carbon in the form of metabolites in a nutritional symbiotic relationship[41]. Such environmental samples present methodological challenges that are comparable to clinical biopsies, as each sample is unique and its history is unknown. In many cases, sample material is limited and can be too small to subsample for additional techniques. Despite sophisticated cell culture models, most sample conditions mimicking colonization and host-specific responses cannot be recreated in the laboratory. Consequently, an in situ analysis of those types of samples is essential.

We therefore developed the metaFISH protocol to combine MSI and FISH on the same tissue section. As a result, we could show that metabolites were associated with bacterial symbionts in the mussel host. Certain host metabolites were absent from colonized cells, and new derivatives of a symbiont metabolite were chemically altered and enriched in host tissue[6]. Finding the site of infection within tissues across whole animals remains a critical challenge. Addressing this challenge, we integrated MSI and FISH with microcomputed tomography to screen for microbial infections and their metabolic fingerprint across organs. We generated a three-dimensional atlas of the metabolic interactions between an invertebrate host, its symbiotic bacteria and tissue parasites[40].

In parallel to our development of metaFISH, advances in spatial resolution were made on the side of MALDI–MSI technology[21,22,42,43]. For example, the introduction of postionization with

Protocol

a second laser (MALDI-2) (ref. [43]) can drastically increase signal intensities for many classes of metabolites. Allowing for smaller ablation spots[21], this innovation has brought MALDI(-2)–MSI to the subcellular level with pixel sizes below 1 μm.

The current technological capabilities of MALDI–MSI, in combination with the advances in sample preparation and handling, now allow the application of metaFISH down to a few individual bacterial cells in tissues. This will be relevant for most host–microbe interactions as we begin to reveal the functional diversity of bacterial microcolonies in symbiosis[44] and pathogenesis[45]. We validated the compatibility of our approach with cutting edge, single-cell resolution hardware, and ensured that metaFISH is not limited to specialized laboratories, by showing its application on widely available commercial MSI systems. The here-presented metaFISH protocol will allow users to generate a correlative dataset that integrates chemical and taxonomic imaging data at scales down to bacterial microcolonies, relevant to host–microbe interactions. The combination of MALDI–MSI and FISH microscopy enables researchers to analyze the spatial metabolomes of diverse host–microbe systems, for example, human biopsies of bacterial infections, symbiotic organs of invertebrates or metabolic microniches that shape the microbiome.

Overview of the protocol

MetaFISH, the spatial visualization of metabolites and microbes at high resolution using MALDI–MSI and FISH consists of sample preparation, imaging and data analysis. The whole protocol can be separated in seven major steps: (1) sampling and tissue embedding, (2) cryosectioning, (3) MALDI matrix application, (4) MSI data acquisition, (5) post-MSI fixation and FISH, (6) fluorescence microscopy, and (7) data handling and integration (Figs. 1 and 2). Key topics that receive special attention include high-resolution MALDI–MSI sample preparation, adjustment of the MALDI imaging parameters (trade-off between MSI signal and material ablation) and postfixation of the sample for FISH. The result of the full workflow will be a combined dataset with co-registered spatial metabolomics data from MSI and host–microbial cell distributions from microscopy of the FISH signals (spatial microbiome data).

As MALDI–MSI damages the tissue, an optimal balance between MALDI–MSI and FISH signal intensities cannot always be achieved. Alternatively, MSI and FISH can be applied independently on consecutive (adjacent) tissue sections following the corresponding sections (Steps 17–27 and 33–49) of this protocol. Additional information such as metabolite annotation derived from the MS data can be integrated.

Applications

In this protocol, we focus on MALDI–MSI and the fluorescent labeling of noncultivable, environmental host–microbe systems that can present methodological challenges, in terms of sample size, traceability and manipulation, comparable to biopsies in humans.

The metaFISH protocol was successfully applied to earthworms[40] and *Bathymodiolus* mussels[6], which both host a defined community of symbiotic bacteria. Studies with similar imaging approaches have focused on natural products in host–microbe interactions and revealed antimicrobial compounds produced by specific bacterial cells on the surface of a beewolf wasp cocoon[39] and co-localized bioactive compounds and bacteria in marine sponges[46].

Future applications of metaFISH could include a broad range of host–microbe interactions from environmental to medical research. This could reveal metabolites produced by pathogenic bacteria as well as the host's immune defense in situ[47]. Besides imaging the distribution of native metabolites, imaging xenobiotics is already applied in pharmacodynamics studies[48]. Here, MALDI–MSI in combination with FISH could detect administered antibiotics around bacterial infection sites[49] and the in situ metabolic phenotypes of the responding bacteria.

The application of metaFISH is not limited to interactions between a few species but can be applied to complex microbiomes as well. Since the selectivity of FISH is based on probe choice, the selected binding sequence of the probe can be as broad as targeting all eubacteria[50] or as specific as individual subspecies[51]. The presented approach could link metabolites to specific members of the gut microbiome. The distribution of metabolites in the gut was shown previously and spatial taxonomic data as provided by metaFISH would be a valuable addition[3,52]. Other interactions that do not involve bacteria but fungi or protists can be studied by using
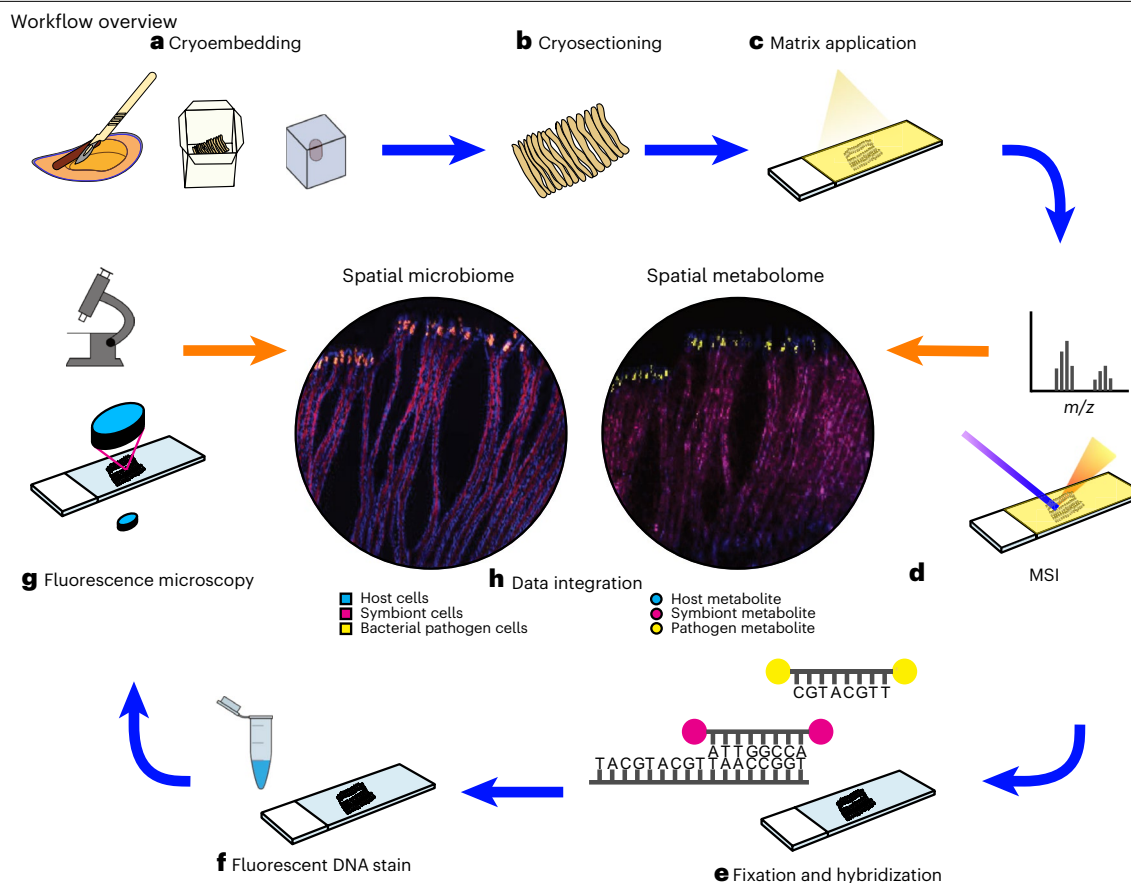
Protocol

Fig. 1 | Workflow for visualization of metabolites and microbes at high spatial resolution using MALDI–MSI and in situ fluorescence labeling (metaFISH). Combining spatial metabolomics and taxon-specific labeling in a correlative imaging and analysis pipeline. **a**, Cryoembedding of tissue sample. **b**, Cryosectioning and transfer on a microscopy slide. **c**, MALDI matrix application. **d**, Measuring metabolites with high-resolution (pixel size <10 μm) MSI. **e**, Tissue fixation, matrix removal and FISH after MSI on the same tissue section using rRNA probes for two phylotypes of bacterial species (magenta and yellow). **f**, General fluorescent DNA staining (blue). **g**, Analysis of the section with fluorescence microscopy. **h**, Final, correlative data integration for spatial metabolome and microbiome results. MSI data shown from AP-SMALDI-5 AF, 10 μm pixel size, sDHB matrix.

18S rRNA specific probes[53,54]. We showed that rRNA can be sufficiently preserved during MSI for subsequent hybridization with probes, other nucleic acid targets are probably compatible. Beyond the taxonomic identity based on rRNA, FISH can be used to target specific genes (geneFISH[32]) and transcripts (mRNA FISH[55]) as well. Combined with MALDI–MSI, mRNA FISH and geneFISH could link metabolites to the presence or expression of a gene.

Limitations

In this section, we address the requirements to carry out this protocol successfully. In general, it is required to achieve intact tissue sections with low topology and to ensure sufficient ionization of target metabolites for MSI. For FISH, the careful design of specific FISH probes and choice of fluorophores is critical for correct taxonomic identification and good signal-to-noise ratio.

Tissue preservation and preparation

For most animal tissues, it is possible to create cryosections compatible with this protocol with adjustments to, e.g., cryotome temperature and embedding media composition. Very hard samples such as bones, stony corals or lignified plant material might require specialized hardware such as tungsten carbide blades, which have been successfully applied to section pig bones[56]. Other samples, such as silicious marine sponges with a high water content and hard silicate spiculae, have so far been deemed unsuitable for cryosectioning[57]. Different
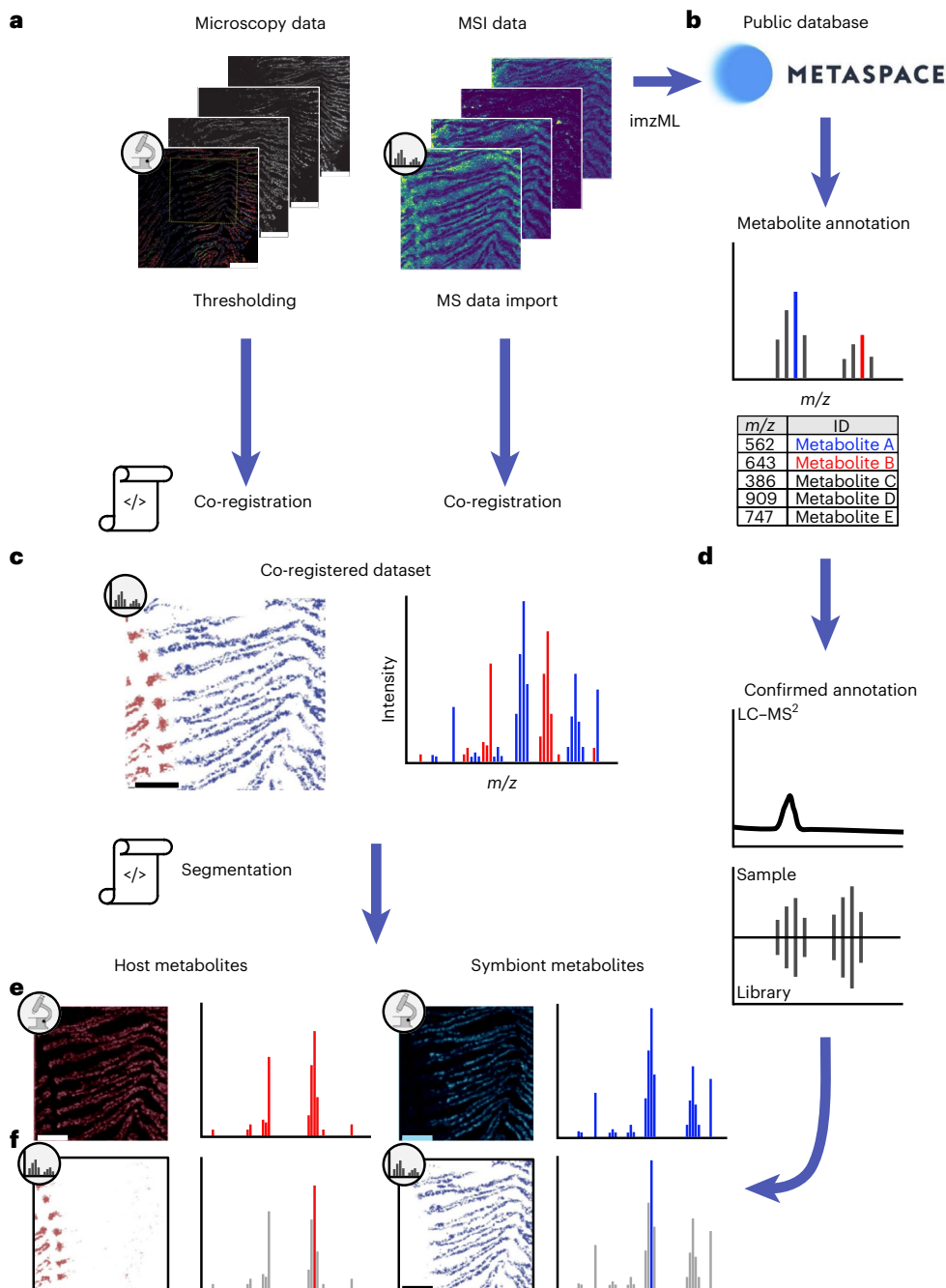
Protocol

Fig. 2 | Combined analysis of spatial metabolome and microscopy data to associate metabolites to host or microbes.
a,b, Starting with fluorescent microscopy and MSI data, consisting of fluorescent channels and ion maps (**a**). Raw data of both modalities needs to be converted into a format suitable for downstream analysis. For fluorescent microscopy, image intensities are thresholded. Depending on the software, MSI data might have to be centroided and converted into the open imzML format (**b**), if vendor formats are not supported. Microscopy images and MSI ion maps are then aligned by co-registration to form one data matrix. **c**, Ion maps and mass spectrum showing both host metabolites in red and symbiont metabolites in blue. Subsequently MSI data is segmented (for details, see 'Data handling') for an unbiased detection of metabolite clusters that correlate with fluorescent signals from the microscopy data. **e**, Host fluorescent signals in red and symbiont signals in blue with associated peaks in the mass spectrum indicated in the same color. Optionally, MSI data can be uploaded to METASPACE for data sharing and metabolite annotation. **d**, Since this annotation is only based on MS[1], it is important to confirm it with other analytical techniques such as LC–MS on tissue extracts. **f**, Ion maps of annotated metabolites associated with host or symbiont as the final data product of metaFISH. Panels **a, c, e** and **f** adapted from ref. 6, Springer Nature Limited.

Protocol

densities of the tissue make it difficult to prepare flat sections, which are important to maintain laser focus during MALDI–MSI for an even energy deposition across the sample. However, uneven samples can be measured with autofocus devices[58]. This effect is pronounced in samples with a heterogeneous composition consisting of liquid-filled vacuoles and hard materials containing chitin, cellulose or bone.

Ionization

Metabolites ionize differently in MALDI–MSI experiments depending on their physio-chemical properties and their interaction with the matrix. Numerous matrices have been investigated since the invention of MALDI, which perform differently depending on sample type, metabolite class, ionization mode and available hardware[59,60]. Pilot tests might be necessary to find a suitable matrix for the target metabolites. The two matrix examples presented here (2,5-dihydroxybenzoic acid (DHB) and 2,5-dihydroxyacetophenone (DHAP)) cover a broad range of metabolites in positive ionization mode. We show that higher laser intensities can generate higher ion signals, but this comes at the expense of tissue ablation and a direct signal reduction for FISH. Considerably higher signal intensities can be achieved for some metabolites with postionization by a second laser (MALDI-2) (refs. [21,43]). Using complementary positive and negative ionization modes is another option to broaden the range of detectable metabolites. Here matrices such as 1,5-diaminonaphthalene or 9-aminoacridine are better suited[61–63]. For molecules that ionize poorly, an additional step such as derivatization with coniferyl aldehyde or 2-picolylamine might be required[47,64–66]. So far metaFISH has not been tested on derivatized MSI samples.

Matrix application technique

Matrix crystal size is a limiting factor for spatial resolution. When single matrix crystals are bigger than the laser spot, this crystal and all integrated metabolites are ionized at once, creating false information for the original metabolite localization in the tissue. Additionally, analyte delocalization can occur during matrix application. Analyte molecules could dissolve and diffuse within the wetted area, as was observed with matrix spraying[67]. To obtain accurate results in high-resolution MALDI–MSI experiments, it is important to carefully control the quality of the matrix by considering both analyte delocalization and extraction efficiency[68]. For the presented metaFISH protocol, we provide examples for suitable matrix application, spraying DHB and sublimation of DHAP.

FISH probes

It is possible to design FISH probes that hybridize with any sequence of typically ~20 bases of DNA or RNA. However, each FISH probe sequence should be tested in silico for specificity to ensure the hybridization will only occur with the target organism and that the binding site is accessible to the probe. If no single probe can be exclusively designed to identify the target organism, multiple probes can be used to resolve different species at the expense of available fluorescent channels for other targets[38,69]. For the presented protocol, we relied on probes that specifically bind to conserved regions of the 16S rRNA of the methane- and sulfur-oxidizing symbionts and the intranuclear, parasitic bacterium. Notably, we commonly use general probes to identify the location of bacterial cells in tissues. For instance, using eubacterial (EUB 338 (ref. [70])) probes allowed us to locate the symbiotic bacteria and the associated metabolites in an earthworm and to extract the site-specific DNA for genome sequencing and taxon identification[40].

Instrumentation

Next to the discussed requirements on sample preparation, the achievable spatial resolution of the MSI dataset is dependent on the available instrument. To distinguish metabolites with very similar masses (isobars) without additional separation technique, a high mass resolution is required. Depending on mass detector technology, the theoretical mass resolution for MALDI–MSI ranges from 10^4 for axial time-of-flight (TOF) devices (e.g., 45,000 at m/z 400 for a rapifleX instrument, Bruker Daltonics) and orthogonal-extracting Q-TOF instruments (e.g., 60,000 at m/z 400 for a timsTOF fleX, Bruker Daltonics), over 10^5 for orbitraps and multi-reflecting TOFs (e.g., 240,000 at m/z 200 for a Q Exactive HF, Thermo Fisher Scientific or 200,000 at m/z 400 for a Select Series

Protocol

MALDI, Waters) to 10^6 for ion cyclotron resonance (>10,000,000 at m/z 400 for solariX, Bruker Daltonics). Imaging with high mass resolution requires longer acquisition times per pixel; a reasonable trade-off between mass resolution and acquisition time is 1 s per pixel or lower (Table 1). The detectable mass range of the instrument has to be considered as well. Ions with very low or high m/z values might not fall into the detection mass range of a given mass spectrometer.

Fine-scale heterogeneity of tissues and microbiomes requires a technique that will work on the same tissue section, as the community and associated metabolomes can change within micrometer scales. Within the thickness of a tissue section, structures such as intracellular communities of microbes can vary drastically. In terms of spatial resolution, commercially available setups offer 5 µm pixel size (e.g., AP-SMALDI-5 AF, timsTOF fleX MALDI-2 with microGRID technology), with smaller pixels so far only been achieved on experimental instruments[21,22]. Single-cell resolution is, however, not a requirement for a successful application of this protocol[40]. Conclusive data can therefore also be generated at lower resolution, as long as metabolite distributions across a tissue can be spatially correlated with infection sites.

Sample throughput

One bottleneck for achieving a high throughput using this protocol is the speed of MSI data acquisition, since a full mass spectrum has to be recorded for each pixel. Current MSI setups have acquisition rates between 1 and 10 pixel s^{-1} (Table 1). Trapping instruments (orbitrap MS, Fourier-transform ion cyclotron resonance (FT-ICR) MS) require longer injection times for higher resolving power. Large area or multisample measurements at high spatial resolution will require long acquisition times (Table 1). Considering the time required for sample preparation, fixation, hybridization and microscopy, analyzing more than two full metaFISH datasets per 24 h period will be challenging in most laboratory environments. A sample throughput of 10 s or more samples per week could be achieved with an MSI setup running 24/7 in combination with the use of automated slide scanning microscopes and data analysis pipelines.

Metabolite annotation

Annotation of metabolites in bulk samples is generally based on accurate mass, comparison with databases and distinct fragmentation patterns in MS^2. In addition, MS is often combined with information from a second dimension such as retention time from chromatography[71,72]. In MSI, the chromatography is exchanged for spatial acquisition, which uses for untargeted metabolomics MS^1. While MS^2 on tissue is possible, ion abundances in targeted MS^2 mode are often not high enough to generate full MS^2 spectra. The required signal intensity for a successful on-tissue MS^2 experiment is highly dependent on the analyte. In the *Bathymodiolus* system, signal intensities ~10×10^4 were still sufficient to conduct fragmentation experiments with the atmospheric-pressure scanning-microprobe matrix-assisted laser desorption/ionization imaging source (AP-SMALDI-10) system. We used a scanning approach over an area of tissue to detect the characteristic fragmentation patterns of specific bacterial lipids when certain bacterial microcolonies were hit by the laser[6]. If the metabolite distribution across a tissue is very heterogeneous, various empty spectra for the target metabolite will be recorded. Apart from fragmentation, a valuable resource for MSI data metabolite annotation is the platform at www.metaspace2020.eu. This platform uses high-mass resolution MS^1 data and metabolite databases to generate a list of possible molecular annotations including a value for the false discovery rate[73]. We advise using bulk metabolomics by liquid chromatography (LC)–MS^2 to complement MSI datasets and identify metabolites with a second technique. Alternatively, ion mobility separation in the mass spectrometer (available, e.g., with the timsTOF fleX; Table 1) is a tool to provide additional information about the identity of isobaric compounds[74]. Be aware that imaging with ion mobility increases measurement time. Annotation with the highest level of confidence usually involves chemical standards, which are measured under the same conditions (e.g., spotting standards on slides, possibly on tissue[75,76]).

Experimental design

One key question for designing an experiment using metaFISH is: what is the location and density of bacterial load within the host and how does this affect the cellular metabolism of the

Protocol

host? While in laboratory models the infection site and approximated bacterial loads are known, patient- or animal-derived samples have to be characterized before metaFISH analysis.

Without previous knowledge about the histological structures of interest such as a symbiotic organ (e.g., the gill in *Bathymodiolus* mussels containing high loads of bacterial cells), additional experiments have to be performed to localize colonization sites (see also 'Troubleshooting'). For samples with an unknown microbial community composition, metagenome sequencing is advised to select suitable and specific 16S rRNA FISH probes[77]. We suggest preserving parts of a sampled organ for additional analyses, e.g., half a tissue/organ stored in a suitable nucleic acid-preserving fixative for metagenome sequencing, with the other half cryopreserved for MSI and FISH.

The infection site can be localized in a tissue sample using general bacterial probes for low-diversity systems or specifically designed FISH probes in complex microbiomes. It is advisable to start with an overview MS image using a lower spatial resolution (10–25 µm pixel size)[39]. This will give guidance in selecting regions of interest (ROIs) to be imaged with high resolution, which will be more time-consuming. To infer that an observed metabolite distribution is representative of a biological system, several specimens should be compared. For statements about relative abundances of metabolites, we suggest including technical replicates, such as consecutive sections prepared and analyzed in the same way.

An uninfected specimen can be used as a control to identify metabolites that differ between healthy and infected host tissue. Metabolites not detected in these controls can be assigned to the infection in the experimental group. This control experiment can be difficult or impossible for environmental samples, e.g., if no animals or samples exist that are free of symbionts (i.e., in obligate symbioses). As for the tissues of the symbiotic deep-sea mussels, we aimed to compare colonized tissues with bacteria-free tissue of the same gill organ to identify metabolites that were specific to the host–microbe interface. We suggest to also measure embedding medium as a control area, which has been sectioned and treated exactly like the tissue samples. This will provide MS features that one can define as background during data analysis of the tissue samples[78].

Experimental design for FISH includes tests for unspecific binding of the FISH probes. Here 'nonsense' probes that have no complementary target can be used as a negative control, indicating unspecific binding with a different fluorophore. Alternatively, tests can be done on a separate tissue section. Additionally, we suggest using formalin-fixed, paraffin-embedded tissue sections that were processed for histology following a 'gold standard protocol' as a positive control for FISH and sample preservation in general.

Expertise needed to implement the protocol

With the above information provided, it is possible to apply the workflow to a broad range of sample types. In case the instrumentation is not available in the executing laboratory, MS and histology or microscopy core facilities may be involved. The required expertise in MSI and fluorescent microscopy does not go beyond what is needed for standard workflows and should be available in any laboratory that uses the respective devices. A team including MS and microscopy trained persons is a good choice to implement the workflow, if there is no single person who has previous knowledge in both fields. Our protocol enables researchers to either do the measurements themselves after training on the machines or communicate sample preparation and imaging parameters to respective core facilities.

Comparison with other methods

There are several ways to perform spatial metabolomics across different scales like the MSI-based microscopic approach presented here, focusing on cellular resolution or macroscopic approaches that look at metabolite distributions across a plant[79]. Common to each approach is the requirement of mapping the chemical data to known structures, such as anatomy, histology and single cells. On an organ level, a software called 'ili' has been released[79], which allows mapping of metabolites measured with liquid chromatography MS (LC–MS) onto three-dimensional datasets, for example, to create a cartography of the microbiome and metabolome of the human lung imaged with magnetic resonance imaging[80].

Protocol

For measuring spatial metabolomes in depth, it has been demonstrated how to excise areas from specific tissue regions for LC–MS-based metabolomics using laser capture microdissection[81]. For following-up on fine-scale chemical gradients in tissues rather than specific histologic features, MALDI–MSI has been used to guide more sensitive LC–MS measurements[82].

Comparable to knowing which organ and tissue was sampled for LC–MS, for single-cell spatial metabolomics it is important to know the cellular environment and identity of the measured cells. Recently, a sophisticated approach was presented to correlate histologic and pathologic states of single cells based on cellular morphometry, with the in situ production of metabolites using histologic stains (H&E) after MALDI–MSI on the same tissue section[83].

More difficult is the identification of fine-scale metabolic heterogeneity in tissues, including the identity of single cells after MSI, to link metabolic state and cellular identity. In one example, a pipeline applied multiplexed immunohistochemistry and MALDI–MSI on the same tissue section to identify immune cell types through image correlations that cannot be distinguished by morphology alone[84]. For identifying cellular heterogeneity within cultured cells, several applications demonstrate how to segment and identify fluorescently transfected single cells and correlate them with their respective metabolomes[14,15,18].

Beyond resolving the heterogeneity of a single organism's tissue or clonal cell populations, using correlative chemical imaging to resolve multispecies associations and their metabolic interactions across scales provides a particular challenge. For example, fluorescence microscopy and MALDI–MSI was used to study biomarkers and drugs in tissues, infected with *Mycobacterium tuberculosis*[85]. In a host–pathogen model, GFP-tagged *Staphylococcus aureus* was used to trace the formation of abscesses in mice and visualize the heterogeneous use of siderophores for iron acquisition by the pathogen in the tissue[86]. One advantage of FISH is the in silico design of probes compared with time-consuming and complicated steps such as antibody production or genetic manipulation to introduce fluorescent proteins.

In summary, substantial advances in sample preparation, imaging protocols and analysis software have been made, linking cellular identity with in situ metabolite production through the combination of fluorescence microscopy and MSI. Our detailed protocol focuses on the spatial localization of nonculturable microbes with FISH that colonize eukaryotic tissues and the associated in situ metabolite production from the same or neighboring tissue section through high-resolution MALDI–MSI.

Combining fluorescence microscopy and MALDI–MSI is particularly powerful. Fluorescent labels reveal single bacteria in tissues and are essential to compensate for MALDI currently not being able to resolve single bacterial cells. This aids the interpretation of the multiplexed, lower spatial resolution MSI data.

Although we focus on MALDI–MSI and FISH, this protocol can serve as the basis for many labeling approaches, such as antibody or bioorthogonal labeling of bacteria via click chemistry[29], used on tissue sections.

Materials

Biological tissues
- Fresh or frozen tissue samples. In the protocol, we use gill samples from deep-sea mussels; the protocol can be adapted for use with other tissue types and organisms. We chose symbiotic *Bathymodiolus* mussels, which host a defined community of symbiotic bacteria in their gills, as well as, in some cases, an intranuclear bacterial parasite. Refer to the 'Troubleshooting' section for a discussion of possible adaptations to other sample types

Reagents
- Sodium carboxymethyl cellulose (CMC) polymer (average molecular weight ~700,000, Sigma-Aldrich, cat. no. 419338) or M-1 Embedding Matrix (Shandon, Thermo Scientific, cat. no. FIS1310)

Protocol

- FISH probes (DOPE-FISH probes, biomers.net, Table 2)
- Formamide (BioUltra, for molecular biology, Sigma-Aldrich, cat. no. 47671)
- Sodium chloride (for molecular biology, Applichem, cat. no. A2942)
- Tris(hydroxymethyl)aminomethane (TRIS; Trizma base, Sigma-Aldrich, cat. no. T1503)
- Hydrochloric acid (HCl; BioReagent, for molecular biology, Sigma-Aldrich, cat. no. H1751)
- Ethylenediaminetetraacetic acid (EDTA) disodium salt dehydrate (suitable for electrophoresis, for molecular biology, Sigma-Aldrich, cat. no. E5134)
- Sodium dodecyl sulfate (SDS; for molecular biology, Applichem, cat. no. A2263)
- DAPI (for nuclear counterstain in immunofluorescence microscopy, Sigma-Aldrich, cat. no. MBD0015)
- Paraformaldehyde (PFA; 20% (wt/vol) methanol-free, Electron Microscopy Sciences, cat. no. 15713)
- PBS (tablets, Sigma-Aldrich, cat. no. P4417) or prepared from NaCl, KCl, Na_2HPO_4 and KH_2PO_4
- 96% Ethanol (vol/vol) (SOLVAGREEN, Ph. Eur., Carl Roth, cat. no. 6724)
- 70% Ethanol (vol/vol), diluted from above with demineralized water
- sDHB with 10% (wt/wt) 2-hydroxy-5-methoxybenzoic acid (Super-DHB, Sigma-Aldrich, cat. no. 50862)
- DHAP (Sigma-Aldrich, cat. no. D107603)
- Methanol (ultra performance LC–MS grade absolute, Biosolve, cat. no. 13684101)
- Acetone (suitable for HPLC, Sigma-Aldrich, cat. no. 34850)
- Deionized water (obtained from Milli-Q Reference A+ water purification system, Merck Millipore, cat. no. Z00QSVCWW)
- Water for FISH probe stocks (Invitrogen UltraPure DNase/RNase-Free Distilled Water, Thermo Scientific, cat. no. 10977049)
- Mounting medium (Vectashield Antifade Mounting Medium, Vector Laboratories, cat. no. H-1000-10)
- Red phosphorus (>97%, Sigma-Aldrich cat. no. 04004)
- Trifluoroacetic acid (TFA; suitable for HPLC, >99.0%, Sigma-Aldrich, cat. no. 302031)
- Dry ice (frozen CO_2)
- Liquid nitrogen

Metabolite standards
Chemical standards for identification and semi quantification of metabolites can be applied next to tissue sections or on the tissue itself[75,76,87]. Standards spotted on tissue help to identify sample specific ion adducts and setup of appropriate MS/MS parameters. Note that some matrix molecules form adducts with metabolites during MS acquisition[78]. If available, extracts of bacterial cell cultures for comparative mass spectral approaches can be spotted next to the tissue[88].

Equipment
- Cryotome (Leica CM3050 S, Leica Biosystems)
- Small paint brush to clear cryotome table (preferred: made from animal hair)

Table 2 | FISH probes used in the protocol example and common general probes

	Target	Name	Sequence 5'–3'	5' Fluorophore	3' Fluorophore	Example
This study	Methanotrophic symbiont	BMARm-845_MOX[102]	GCTCCGCCACTAAGCCTA	Atto 647	Atto 647	Figs. 6 and 8, ref. 6
	Thiotrophic symbiont	BMARt-193_SOX[102]	CGAAGGTCCTCCACTTTA	Atto 550	Atto 550	Ref. 6
	Intranuclear parasite	Bnix1249[103]	GCAGCTTCGCGACCGTCT	Atto 550	Atto 550	Figs. 5 and 8
General	Most bacteria	EUB 338[70]	GCTGCCTCCCGTAGGAGT	Any	Any	Fig. 7, ref. 40
	Archaea	ARCH915[104]	GTGCTCCCCCGCCAATTC CT	Any	Any	—
	Gammaprotobacteria	GAM42a[105]	GCCTTCCCACATCGTTT	Any	Any	—
	Betaproteobacteria	BET42a[105]	GCCTTCCCACTTCGTTT	Any	Any	—

Protocol

- MSI devices (Table 1)
    - AP-SMALDI-5 AF or AP-SMALDI-10 (TransMIT, coupled to Q Exactive HF, Thermo Fisher Scientific)
    - timsTOF fleX MALDI-2 with microGRID (Bruker Daltonics)
    - t-MALDI-2 prototype ion-source (Dreisewerd/Soltwisch Lab, University of Münster, coupled to Q Exactive plus, Thermo Fisher Scientific)
- Matrix application device (Sprayer/Sublimation chamber):
    - SunCollect Micro Fraction Collector/MALDI Spotter (SunChrom)
    - Sublimation chamber prototype built in the Dreisewerd/Soltwisch Laboratory[42]
    - Or commercial sublimation chamber
- Fluorescence microscope (BX 53, Olympus)
- Incubation oven 46 °C (UVP HB-1000, Ultra-violet Products)
- Heated water bath 48 °C (Thermolab 1070, GFL)
- 50 ml conical tubes (Eppendorf, cat. no. 0030122178)
- 2 ml tubes (Safe-Lock Tubes Biopur, Eppendorf, cat. no. 0030121597)
- 0.5 ml PCR tubes (PCR clear, Eppendorf, cat. no. 0030124537)
- Cryomolds (Peel-A-Way Disposable Embedding Molds, Polysciences., cat. no. 18646A-1)
- Microscopy slides:
    - Polysine slides (Epredia, Thermo Scientific, cat. no. 10219280)
    - Indium tin oxide-coated slides for t-MALDI (Sigma-Aldrich, cat. no. 576352)
    - IntelliSlides with teachmarks for automated co-registration (Bruker Daltonics, cat. no. 1868957)
- White paint marker (Edding 751)
- Red Marker (Edding 140 S)
- Liquid blocker (Super PAP Pen, Science Services, cat. no. N71310-N)
- Dewar for liquid nitrogen, protective gloves
- Insulated box for dry ice
- pH meter

Software
- Acquisition software for MSI (vendor dependent)
- Acquisition software for microscopy (vendor dependent)
- Software for MSI data analysis:
    - Commercial software: SCiLS Lab (Bruker Daltonics) Version 2020b (or higher), with Pro and MVS package
    - Mirion 3D Version 3.3.64.17 (ref. [89])
    - Open-access software: Rstudio and Cardinal package[90], MATLAB (MathWorks) for scripts provided under Step 26
- Software for MSI data conversion:
    - MSconvert GUI Version 3.0.9810 (ProteoWizard, download from http://proteowizard.sourceforge.net/download.html)
    - imzML Converter version 1.3.0 (ref. [91]) (download from https://github.com/AlanRace/imzMLConverter)
- Metabolite annotation:
    - METASPACE (www.metaspace2020.eu)[73]
    - Lipostar2 and LipostarMSI (Molecular Discovery)[92,93]
    - MetaboScape (Bruker Daltonics)

Reagent setup
Tissue samples
Prepare directly from fresh specimen or from snap-frozen tissue stored at −80 °C. All samples need to be untreated, i.e., no chemical alteration such as fixation with formaldehyde, nucleic acid preservative infusion or storage in solvents that possibly extract metabolites from the tissue. During field collection, we recommend storing parts of tissues for metaFISH and some parts from the same tissue for DNA or RNA sequencing and bulk metabolomics experiments.

Protocol

▲ **CAUTION** When working with animal and human samples, make sure to follow all applicable ethics and safety guidelines and regulations. Notably, frozen tissues have not been inactivated chemically, through heat or radiation, which has to be taken into account when working with infectious agents.

Embedding medium (CMC gel)

As the embedding medium, a commercially available CMC embedding medium (M1, Thermo Scientific) can be used. Alternatively, for a 2% (wt/vol) solution, dissolve 1 g CMC in 50 ml warm (40 °C) deionized water in a 50 ml tube and vortex thoroughly. To help dissolve the CMC, place the tube in a water bath at 40 °C for several hours or overnight. Shake the tube to make sure crystalline parts dissolve fully, stirring with a clean spatula might be necessary to break up clumps. To remove air bubbles from the gel, centrifuge the tube for 2–3 min at 1,000 g at least. Only use CMC embedding gels that are completely clear and free of big air bubbles. To avoid growth of microorganisms in the prepared gel, store the gel at −20 °C (long term storage) or store at 4 °C if used within the next 1–3 d. Alternatively, the gel can be autoclaved and stored in suitable containers at room temperature (18–22 °C).

MALDI matrix solutions

Prepare fresh before use. It is important to dissolve the matrix completely in the solvent. In cases of precipitation or presence of residues in the solution, it is advised to filter or centrifuge the matrix solution to avoid clogging of e.g., the sprayer capillaries. For spraying DHB matrix prepare a 1:1 solution of methanol in LC-grade water, add TFA to reach 0.1% (vol/vol) in the solution, then dissolve 30 mg ml^{-1} by vortexing. For the sublimation approach with the matrix DHAP, it has also proven advantageous to handle the matrix dissolved in an organic solvent such as acetone. This not only helps with conveniently adjusting the amount of matrix to be sublimated, but also with creating a homogeneous layer in the matrix sublimation reservoir. Stocks of 20 mg ml^{-1} DHAP in glass vials can be prepared.

▲ **CAUTION** Methanol is toxic and flammable, acetone is flammable and TFA is corrosive. Wear gloves and work in a fume hood.

PBS

PBS can be purchased as ready-made solutions or in tablet form, both of which are suitable for the presented protocol. Alternatively, it can be prepared for direct use or as a ten times concentrated stock solution. Add the chemicals to a final concentration of 137 mM NaCl, 2.7 mM KCl, 10 mM Na$_2$HPO$_4$ and 1.8 mM KH$_2$PO$_4$ to 800 ml deionized water in a 1 l glass bottle and dissolve under constant magnetic stirring. Adjust the pH of the PBS solution to 7.4 before filling up to 1 l with deionized water and autoclave the solution at 120 °C for 20 min. See Supplementary Table 5 with weights for 1× and 10× solutions.

2% (wt/vol) PFA in PBS

Appropriately dilute commercial PFA solution with PBS. Alternatively, PFA can be dissolved in deionized water under heating and NaOH addition until clear before adding the appropriate amount of PBS stock solution. However, we recommend using methanol-free PFA to prepare fresh fixation solutions for reproducible results.

▲ **CAUTION** PFA is toxic, wear gloves and work under a fume hood.

Hybridization and washing buffers

The buffers should be prepared fresh before an experiment. It is advisable to aliquot the required reagents into a few stable stock solutions (listed below) that can be stored at room temperature. Many of these standard stock solutions are also available from laboratory suppliers.

5 M sodium chloride solution

Dissolve 292.2 g of NaCl in 800 ml deionized water in a 1 l glass bottle that is filled up to 1 l with deionized water and autoclaved (120 °C, 20 min).

Protocol

1 M TRIS–HCl can be obtained as premade solution. Alternatively dissolve 121.1 g of TRIS base in 800 ml deionized water in a 1 l glass bottle, adjust the pH to 7.4 with 37% (wt/wt) concentrated HCl (~70 ml), fill up to 1 l with deionized water and autoclave (120 °C, 20 min).

▲ **CAUTION** HCl is corrosive, wear gloves and work in a fume hood.

10% (wt/vol) SDS
Dissolve 10 g of SDS in 90 ml sterile (autoclaved) deionized water in a 250 ml glass bottle (wear a mask when weighing SDS). Heat to ~70 °C to assist liquefaction. Adjust the pH to 7.2 with HCl and fill up to 100 ml with deionized water.

0.5 M EDTA (pH 8.0)
This can be obtained as a premade solution. Alternatively, add 186.1 g of disodium ethylenedia minetetraacetate*$2H_2O$ to 800 ml deionized water in a 1 l glass bottle. Stir on a magnetic stirrer and adjust pH to 8.0 with NaOH (~20 g of NaOH pellets). Fill up to 1 l with deionized water and autoclave (120 °C, 20 min).

▲ **CAUTION** Sodium hydroxide is caustic, wear gloves when handling.

Hybridization buffer
The buffer is made from the previously described solutions. Combine the prepared stock solutions in 2 ml tubes to final concentrations of 900 mM NaCl, 20 mM TRIS, and 0.01% (wt/vol) SDS. Add the SDS stock solution last to avoid precipitation. The concentration of formamide depends on the used FISH probes and ranges from 0% to 60% (vol/vol). See Supplementary Information for volumetric tables for the hybridization buffer.

▲ **CAUTION** Due to the volatile nature and toxicity of the compound, handle formamide-containing solutions on ice.

Hybridization mixture
Prepare just before the hybridization step to minimize the exposure to room temperature and to light. Add FISH probes to a final concentration of 5 ng μl^{-1} to the hybridization buffer in a PCR tube and mix by pipetting up and down a few times. Prepare enough hybridization mixture to cover the entire tissue sections (e.g., 30–50 µl per section of ~5 × 10 mm^2, or 1 µl mm^{-2}).

FISH probes
FSH probes are supplied in a freeze-dried form and must be dissolved in PCR water to a concentration of 100 pmol μl^{-1}. Probe stocks are stored frozen at −20 °C and only thawed briefly to prepare fresh hybridization mixtures. Avoid exposure to sunlight to prevent fluorophore bleaching.

Washing buffer
Make in a 50 ml tube by combining the prepared stock solutions to final concentrations of 20 mM TRIS, 0–900 mM NaCl. At more than 20% (vol/vol) formamide concentration in the hybridization buffer, 5 mM EDTA should be added. The stringency in the washing buffer is modified by adjusting the NaCl concentration, which avoids the use of excess amounts of formamide. See Supplementary Table 4 of NaCl concentrations according to the formamide concentration of the hybridization buffer. Add 0.01% (wt/vol) SDS last to avoid precipitation.

Equipment setup
Calibration of mass spectrometers
Calibration is performed according to the manufacturer's instructions. In the case of the AP-SMALDI-5 AF and AP-SMALDI-10 source mounted to Q Exactive (Thermo Fisher Scientific) mass spectrometers, a mass calibration is carried out using matrix-derived ions before each measurement[94]. Alternatively red phosphorus can be used for mass calibration in positive and negative mode[94,95], which is the standard procedure on timsTOF fleX devices. Further calibrations of the MS settings should be done according to the manufacturer's guidelines with the HESI source attached. Usage of a lock mass during image acquisition is advised. Matrix-derived ions have been proven to provide stable signals for this purpose[94].

Protocol

Cryotome, hybridization oven and water bath
They should be set to the target temperature for at least 30 min before use, such that temperatures have stabilized when work begins.

Procedure

Tissue preparation, cryoembedding and cryosectioning

● **TIMING** 2–3 h (depending on experience level and number of sections cut)

1. Separate mussel shells by cutting through the adductor muscle with a scalpel. Separate the gills from other tissues and cut out a sample a few millimeters across.
2. The tissue sample can be stored frozen at −80 °C or embedded directly and then stored at −80 °C.
3. For embedding, fill a cryomold with precooled (4 °C) 2% (wt/vol) carboxymethyl cellulose gel (see 'Reagent setup') by slow pouring.
4. Use cut-off plastic pipettes to pipette out all air bubbles from the mold.
5. Gently push a frozen gill tissue sample into the center of the mold with tweezers.
   ▲ **CRITICAL STEP** Note the orientation of the tissue within the block and mark one corner of the plastic mold. After freezing, the CMC block will be opaque and it is often not possible to determine the tissue orientation for the intended sectioning plane.
   ◆ **TROUBLESHOOTING**
6. To freeze the sample, hold the cryomold with tweezers and dip it briefly into liquid nitrogen so that the bottom of the mold touches the liquid surface; unidirectional freezing from bottom to top gives the best results.
   ▲ **CAUTION** Liquid nitrogen can cause skin burns. Wear protective gloves and goggles while handling.
   ■ **PAUSE POINT** Frozen CMC blocks can be stored on dry ice during preparation or at −80 °C for several months. Store samples in vacuum bags or sealed containers with a minimum volume of air to prevent freezer burn and possible oxidation of the sample.
   ◆ **TROUBLESHOOTING**
7. Mount the sample block by pressing it on a small amount of optimum cutting temperature (OCT) mounting medium applied to the sample holder in the cryotome (Fig. 3a).
   ▲ **CRITICAL STEP** Ensure the correct orientation of the embedded sample to obtain a section perpendicular to the filament orientation, not along them.
8. Let the sample harden and acclimatize for a few minutes.
   ▲ **CRITICAL STEP** Avoid getting OCT on surfaces intended for MSI as this polymer introduces high background signals.
9. Use a single-edge safety razor blade to trim the CMC in a truncated pyramid shape (Fig. 3b–d) around the embedded sample, as known from classical histology/electron microscopy. Leave a few millimeters of CMC around the tissue.
10. Section tissue to 6–10 μm thickness with a cryostat at a chamber temperature of −35 °C and temperature of the object holder at −22 °C for soft invertebrate tissue with a high water content.
    ▲ **CAUTION** Cryotome blades are extremely sharp, only use a brush to remove shavings from the blade. Lock the cutting mechanism when working inside the cryotome. Avoid prolonged contact with metal surfaces in the cryotome chamber to prevent cold burns.
    ▲ **CRITICAL STEP** At temperatures below −40 °C, CMC is extremely brittle. If samples have been stored at −80 °C, move them to −20 °C for at least overnight before sectioning.
    ◆ **TROUBLESHOOTING**
11. Carefully move tissue sections with a thin paint brush at cryotome chamber temperature. Some folding might be remedied by careful prodding with the tip of a brush.
12. Once a suitable tissue section without breaks is achieved, thaw-mount it on polylysine coated slides.
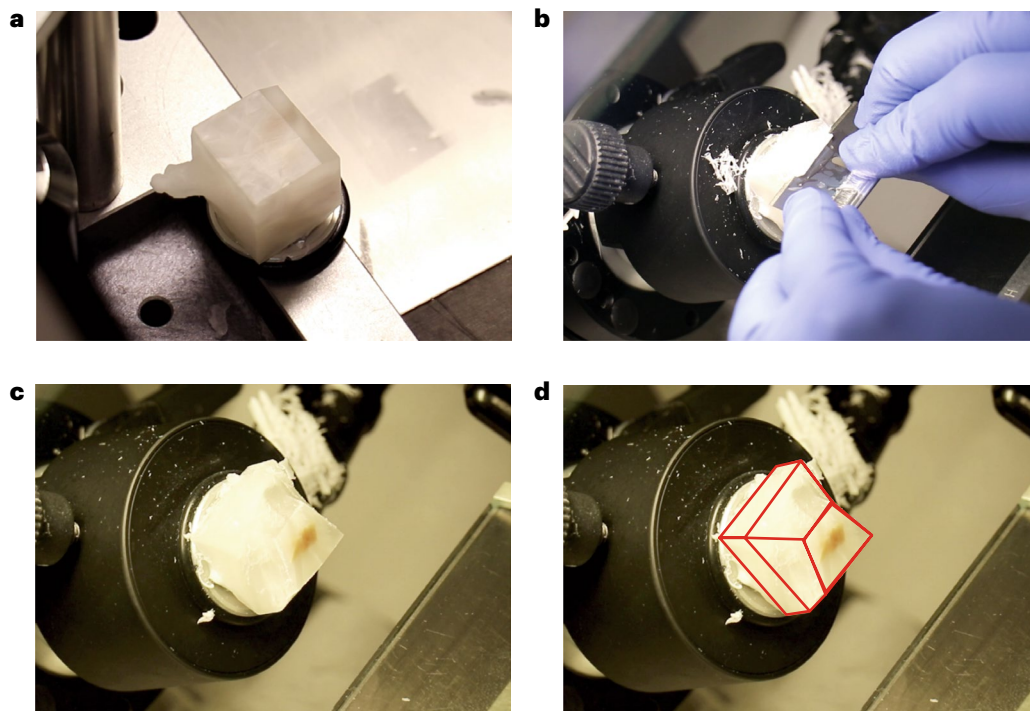
Protocol

Fig. 3 | Trimming of CMC block before cryosectioning. To obtain good tissue sections, trimming of the CMC block with cryoembedded tissue is crucial. **a**, Step 7, mounting the tissue block in the correct orientation to section in the desired plane. **b**, Step 9, trimming of the CMC block with a razor blade into a 'truncated pyramid' shape. **c**, A tissue block ready to be sectioned. **d**, Outline of the ideal shape of the CMC block for sectioning (indicated by red lines). Note the few millimeters of CMC left around the embedded tissue as well as the broad side of the trapezoid cross-section of the side facing the cryotome blade after completing Step 9.

13. Move a microscopy slide at room temperature toward the tissue section, facing it with the coated side. The tissue section will adhere to the slide and thaw. Placed at room temperature, the section will dry in a short time.

    ▲ **CRITICAL STEP** Warming the glass slide by keeping it in the hand after taking it out of the cryotome prevents condensation of ambient humidity.

    ■ **PAUSE POINT** If samples are not processed further right away, store samples at −80 °C or in a vacuum desiccator at room temperature. To prevent condensation during thawing, store frozen slides with tissue sections in sealable slide containers with silica granules or vacuum bags.

    ◆ **TROUBLESHOOTING**

Marking and microscopy
● **TIMING** 30 min
14. If stored frozen, allow slides to reach room temperature in the slide containers before this step to prevent water condensation due to ambient humidity.
15. Mark the glass slide very close to the tissue with small dots of white paint for orientation after matrix deposition. Place a dollop of paint (e.g., from an Edding 751) on a separate glass slide and use a short hair (e.g., eyebrow or animal hair) attached to the tip of a toothpick to create a single-tip paintbrush and make small markings next to the tissue. Those marks with white ink are fiducial markers that can be used for orientation in bright-field microscopy, MALDI–MSI and fluorescence microscopy.

    ▲ **CRITICAL STEP** Small dots of paint leave a structure that can be seen even after an opaque matrix has been deposited and the marker has a specific molecular signature and autofluorescence, which can help with the alignment of microscopy and MS images.

Protocol

▲ **CRITICAL STEP** It is essential that the paint marker is insoluble in the organic solvents used to spray the ionization matrix to avoid diffusion into the tissue. The marker (Edding 751) used here works with acetone, methanol, ethanol and acetonitrile.

▲ **CRITICAL STEP** Markings are essential for orientation on the slide with the acquisition software and later co-registration of optical and MSI data. Bruker Daltonics IntelliSlides come with teachmarks for this purpose, for other slides, markings have to be applied manually.

16. Acquire overview images of the prepared slides (Fig. 4a) in bright-field and tissue autofluorescence (488 nm excitation) channels. Overview images of the slides covering tissue sections and markings are essential for orientation and navigation to the often small areas (e.g., specific cells) that will be measured with high-resolution MALDI–MSI.

◆ **TROUBLESHOOTING**

Matrix application and marking

● **TIMING** 1 h

▲ **CRITICAL STEP** For a spatial resolution (pixel size) of 10 μm, spraying DHB according to this step is suitable; for 5 μm pixel size the matrix quality is sometimes insufficient. We recommend applying DHAP by sublimation for measurements with a pixel size below 10 μm (Box 1).

▲ **CRITICAL STEP** Before applying matrix to a sample, an empty test slide should be coated to ensure proper functioning of the matrix application device. To check matrix quality for crystal size and coverage, use a microscope.

17. DHB deposition by sprayer. Deposit ten layers of a 30 mg ml^{-1} solution of DHB (see 'Reagent setup') at a flow rate of 10 μl min^{-1} (layer 1) and 15 μl min^{-1} (layers 2–10) using a SunCollect Micro Fraction Collector/MALDI Spotter (for full sprayer settings, see Supplementary Table 6).

▲ **CRITICAL STEP** A coverage of ~200 μg cm^{-2} is a reasonable value for matrix deposition. Weighing slides before and after matrix application can help to establish suitable and reproducible parameters for matrix application devices.
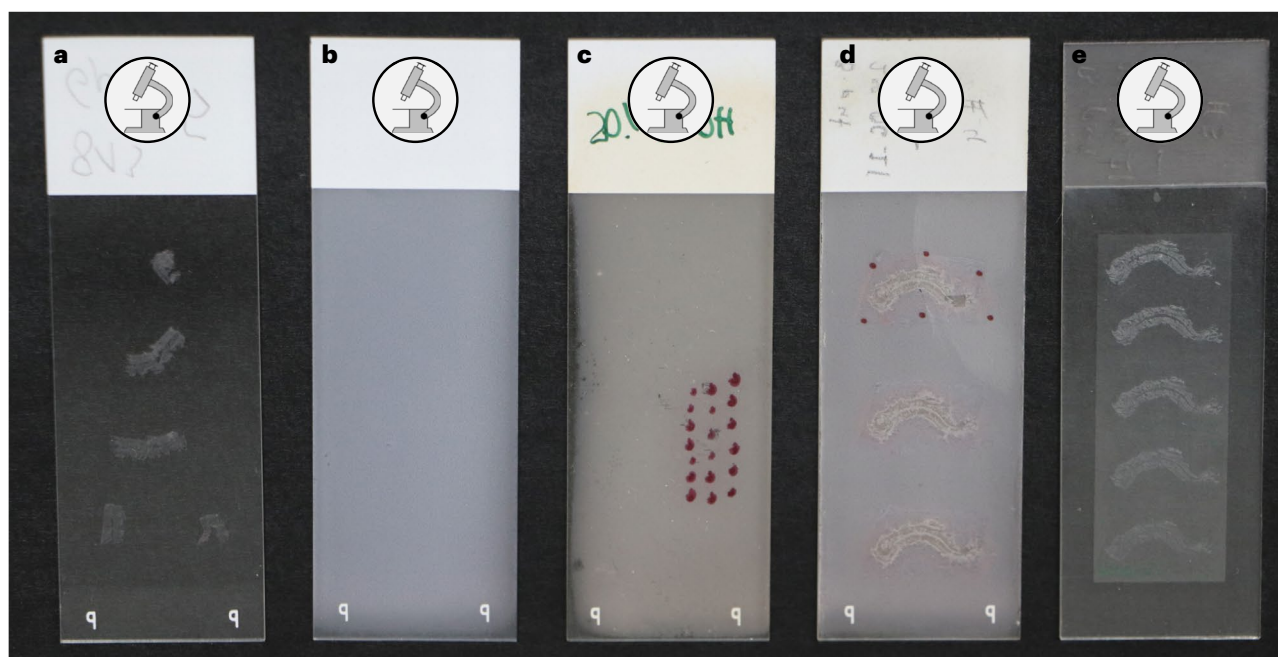

Fig. 4 | Tissue section and microscopy slide documentation to follow the protocol. a, Step 16, after mounting, check if the tissue sections are intact, look out for tears, distorted section or tissue folded in on itself. Sections for subsequent analyses are selected at this step. **b**, Step 18, after matrix application, check for an even coat of matrix and small crystal size. **c**, Step 19, localize the tissue section under the matrix and apply markings around it. Protrusions of white paint markings applied before matrix coating can be helpful. **d**, Step 26, after MSI acquisition, inspect the measured region. At this step, the size of ablation craters and oversampling (no separation between ablation spots) can be observed. Tissue damage by high laser intensities can also be detected at this step. **e**, Step 47, after fixation and hybridization, record an overview image and check if the tissue is still attached to the slide and intact. Also check for air bubbles that can negatively impact signal intensities.

18. Record an overview image of the slide to control matrix quality (Fig. 4b).
    ◆ **TROUBLESHOOTING**
19. If previous markings are poorly visible, apply markings with red marker around the intended measurement area (Fig. 4c).

MSI

● **TIMING 30 min setup plus measurement time (hours to days for very large measurement areas)**
▲ **CRITICAL** The choice of MSI setup in most cases will be based on which device is available in a given laboratory setting. See 'Instrumentation' for a discussion of spatial and mass resolution for different MALDI mass spectrometers. Here, we present generalized instructions for MSI acquisition. Detailed instructions for two commercial and one experimental setup can be found in Supplementary Information (Supplementary Methods 1–3).

20. Place the slide with matrix-coated tissue sections in the sample holder of the MSI setup.
21. If available, use the autofocus function to adjust the stage position in the Z-axis.
22. In any case, manually control for optimal laser focus by shooting the laser at matrix next to the tissue sections while manually adjusting the Z position until the minimum/best ablation spot size is achieved.
23. Repeat this adjustment on all four corners around the selected measurement area to adjust for out-of-plane slide position.
    ◆ **TROUBLESHOOTING**

BOX 1

Matrix application

The matrix and application protocol, which is used for MSI experiments, should be tested for suitability. For matrix sprayers, the flow rate, distance to sample and solvent system can be adjusted to ensure almost instant drying on the slide without large crystals forming. For high-resolution (pixel size <10 μm) MSI measurements, we recommend sublimation over spraying, as also shown by others[106] (Supplementary Method 1). We showed that the matrices and their way of application, such as sprayed CHCA[40], sprayed DHB[6] and sublimated DHAP (this study; Fig. 5) did not interfere with the subsequent FISH analysis after the washing step.

To ensure that the MALDI image represents the spatial distribution of analyte in the sample as well as possible, artifacts during sample preparation have to be avoided. The step with the greatest impact is matrix application. Too wet spraying conditions may lead to diffusion of dissolved analytes as well as bigger matrix crystals. Consequently, diffused analytes will be detected in the periphery of its origin. In addition, for samples with high lipid content with a low melting point such as triglycerides, increased temperatures can lead to a liquefaction and delocalization. To check for preparation artifacts, first acquire a microscope image of the tissue, apply the matrix with the selected preparation method and acquire a small MALDI image with highest possible lateral resolution. Next, co-register both imaging modalities and select some m/z values of metabolites expected to localize only in the tissue. Check whether ion intensities can be observed in areas that do not co-localize with tissue or in the periphery of the tissue. If this is the case, a different sample preparation strategy, for example, using less solvent or matrix sublimation, should be considered.

If analyte delocalization is observed, although matrix sublimation is used, other potential sources of error can, for example, be a too humid atmosphere to which the sample is exposed. Make sure that the sample is at room temperature before venting the vacuum sublimation chamber. Additionally, reduce time between sublimation process and MALDI measurement.

In case sublimation of a MALDI matrix does not deliver homogeneous matrix coating, check the thermal contact of the sample with the cooling unit of the sublimation chamber. Also, make sure that the matrix is spread as homogeneous as possible in the heated matrix reservoir.

The second most common source of analyte diffusion out of the sample, independent of the matrix application, is tissue embedding. To control for embedding-based analyte diffusion in tissue samples, section samples without embedding if possible or ensure that samples remain frozen throughout whole embedding process.

Protocol

24. Next, the laser intensity and number of shots per pixel have to be adjusted (Box 2 and Fig. 5). Select a mass range and ionization mode suitable for the metabolites of interest. Record mass spectra next to the intended measurement area or on a separate section while testing different laser settings, until the optimal settings for high ion intensities are found.

25. Select the area to be measured

26. Start the measurement and wait for data acquisition to complete.
    ◆ TROUBLESHOOTING

27. The generated mass spectral and positional data files are both required for subsequent analysis.
    ■ PAUSE POINT Take out the slide and store under vacuum if not processed further immediately. If more MALDI–MSI measurements are to be performed on the same sample, slides with matrix should not be stored under vacuum to prevent slow sublimation. Use a conventional slide box stored in a dry place instead.

28. Record an overview image after MSI (Fig. 4d) with a slide scanning microscope. Record and measure the distance between ablation spots to verify the MSI resolution and to detect oversampling.
    ■ PAUSE POINT After recording the overview image slides can be stored as described under the previous step.
    ◆ TROUBLESHOOTING

Fixation of samples after MSI

● TIMING 2–3 h

29. Use tissue tips or cotton swabs wetted with 70% (vol/vol) ethanol to carefully wipe away matrix and markings around the tissue with swiping motions away from the tissue towards the edge of the slide. Make sure the cotton swab is not too wet—no liquid should drain onto the slide.
    ▲ CRITICAL STEP Removing most excess matrix and markings before submerging the slide into fixative prevents diffusion of pigments into the tissue.

BOX 2

Laser settings

To determine ideal settings for MSI acquisition, test measurements have to be performed for each sample type. In general, higher laser intensities and more laser shots per pixel will generate more ions and a higher signal intensity in MSI. However, this will result in an increased amount of tissue being ablated (Fig. 5). Tissue ablation leads to the distortion of the tissue morphology as well as to less available nucleic acids for the FISH probes to bind and microscopy signal intensity will decrease. Scenarios where all bacterial cells are ablated can happen but should be avoided. This trade-off between signal intensity and tissue ablation has to be kept in mind when optimizing the MSI setting for metaFISH. It should be noted that different metabolite classes behave differently, some ionize better upon using higher primary laser intensities (e.g., sterols with MALDI-2 (ref. [107])) and some show higher signals using more laser shots per pixel. Postionization with e.g., MALDI-2 increases metabolite signals for a wide range of metabolites[42,108]. The increased sensitivity may allow reducing the amount of ablated tissue/pixel size. We advise to use a range of MSI settings as shown in Fig. 5 to determine an optimal compromise for obtaining high metabolite ion as well as FISH signals.

Particularly in MSI systems that use a high vacuum in the ion source, long measurement times can be problematic as volatile metabolites and matrix can evaporate. In these cases, chemical modifications of the matrix can be introduced to make it less volatile[109]. A general decrease in signal intensity over the course of the measurement should be investigated. Additionally, metabolites can degrade during sample storage[110] and thus potentially during a very long MSI experiment. If a signal decrease over the course of a measurement is observed, it needs to be ruled out that this is the result of metabolite instability in the instrument. A measurement of a fresh sample compared with a measurement after some time in the instrument can help constrain the maximum measurement time.
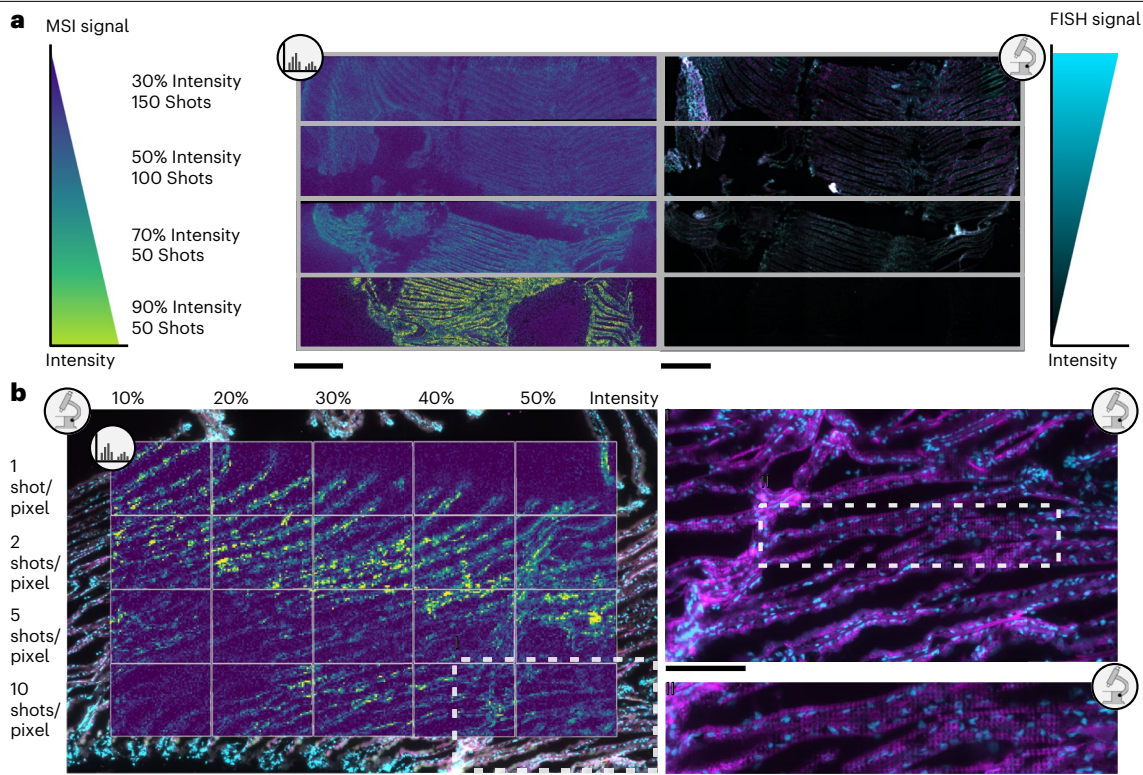

Protocol

Fig. 5 | Laser intensity and shot number influence MSI and FISH signal intensity. Laser intensities correlate to signal intensity for MSI because more material is ablated and ionized. Since FISH relies on intact strands of nucleic acids for hybridization, more material ablation leads to a reduction in fluorescent signal intensity. Laser-induced tissue damage is also reflected in decrease in DAPI signal, which binds to DNA. The samples were measured with a pixel size of 5 μm on a timsTOF fleX MALDI-2 instrument with microGRID and use of different laser settings indicated in the figure. Subsequently the same samples were analyzed by FISH. **a**, Gill tissue section of *Bathymodiolus childressi* with metabolite signal intensity shown on the left using ion maps for 35-aminobacteriohopane-31,32,33,34-tetrol. The [M+H]⁺ ion with *m/z* 563.467 ± 20 ppm is shown in viridis color scheme. On the right, microscopy of FISH signals (magenta: EUB I, general bacteria probe; cyan: DAPI, general DNA stain). **b**, Tissue gill section of *Bathymodiolus puteoserpentis*. Metabolite signal intensity is shown on the left with the ion maps for bacteriohopane-31,32,33,34-tetrol, [M+H]⁺ ion with *m/z* 547.472 ± 10 ppm in viridis color scheme. MSI and FISH overlay is done with composite image of FISH and stain signals (magenta: methanotrophic symbiont; cyan: DAPI). On the right, zoom-in of microscopy data to show laser ablation marks. Scale bars: **a**, 200 μm; **b**, 100 μm.

30. Submerge the glass slide with matrix-covered tissue section in a 2% (wt/vol) PFA/PBS solution for 1 h at room temperature in a 50 ml conical tube.

    ▲ **CAUTION** PFA is toxic, wear gloves and work under a fume hood.

31. Wash off fixative by submerging the slide for 10 min in PBS at room temperature, then repeat the step with fresh PBS for 10 min.

32. Cautiously dip the slide into 96% (vol/vol) ethanol and allow the slide to quickly air dry afterwards.

    ▲ **CRITICAL STEP** Avoid rapid movement of the slide in the solutions, which could cause damage to the tissue sections despite fixation.

FISH

● **TIMING ~3 h**

Generally, thicker tissue sections are unproblematic for FISH and even whole mounts of small animals are possible[96]. In our experience, between 100 and 300 μm can be penetrated by FISH probes (see Box 3). Very opaque tissue might require a tissue clearing step before microscopy[97]. Problems of signal interference can be overcome by using a confocal laser scanning microscope and generating optical sections or *Z*-stacks.

Protocol

33. Prepare the hybridization mixtures according to 'Reagent setup'.
34. Put one piece of folded disposable lab tissue into a 50 ml tube and pipette the remaining hybridization buffer onto it.
35. Close the tube and place it in the hybridization oven. The wetted paper will ensure a formamide–water saturated atmosphere.
    ▲ **CAUTION** Formamide is toxic, wear gloves and work under a fume hood.
    ▲ **CRITICAL STEP** Before choosing the fluorescence dyes for the probes, test the autofluorescence of the tissue. Avoid probes with absorption in the range of the autofluorescence from the tissue, this will result in better signal-to-noise values for the probe signal.
36. Draw a circle around the tissue section with a hydrophobic liquid blocker or use silicone spacers to prevent the hybridization mixture from running off during incubation.
    ▲ **CRITICAL STEP** If different probe mixtures leak and mix on a slide, hybridization can be ruined when the sample and negative control are on the same glass slide.
37. Carefully pipette the hybridization mixture with FISH probes (Table 2) on the tissue sections until fully covered, while avoiding touching/scratching the tissue section with the pipette tip.
38. Carefully insert the slide into the prepared 50 ml tube above the paper and close the lid.
39. Hybridize tissue sections and control samples for 2 h at 46 °C in a hybridization oven.
    ▲ **CRITICAL STEP** Keep the slide and 50 ml tube horizontally at all times to avoid the hybridization mixture running off.
    ▲ **CRITICAL STEP** Put a 50 ml tube with washing buffer into a heated water bath at this step so it is at 48 °C (2 °C above hybridization temperature) when hybridization is complete.
40. Remove the slide from the 50 ml tube and directly place it into the prewarmed washing buffer.
41. Incubate for 15 min at 48 °C in a water bath.
    ▲ **CRITICAL STEP** Unspecific binding of probes can occur if the temperature of the washing buffer drops substantially. Avoid long distances between instruments and keep all required equipment in close proximity.
42. Cautiously dip the slides in PBS (at room temperature) to remove remaining buffers.
43. Subsequently dip the slides in deionized water to remove salts.
44. Finally, dip the slides into 96% (vol/vol) ethanol to reduce the water amount and speed up the drying process.
45. To stain the DNA of host and bacteria with DAPI, pipette 20 mM DAPI solution onto the tissue sections until fully covered.
    ▲ **CAUTION** DAPI is mutagenic, wear gloves and avoid skin contact.

BOX 3

FISH probes

We recommend the use of specific 16S rRNA probes for the target bacteria, labeled with two fluorophores at the 5' and 3' ends of the oligonucleotide, for increased signal intensity (DOPE–FISH)[111]. To further increase the fluorescence signal and allow simultaneous labeling of several bacterial taxa, multilabeled FISH could be employed.

While catalyzed reporter deposition FISH probes[112] offer even higher signal intensities, harsher sample treatment is needed to allow the horseradish peroxidase to penetrate the tissue. Each additional step of the catalyzed reporter deposition FISH protocol such as permeabilizations, activation, inactivation and a second hybridization can lead to tissue damage or dislocation and affect precise image correlations to the MSI data.

To choose suitable FISH probes, visit probeBase (https://probebase.net), which offers an overview of previously published probes. If no published probe for the bacterial species present in a given sample can be found, nucleotide probes need to be designed in silico, as reviewed elsewhere[113,114]. If desired, use a negative control probe (see table/sequence) for unspecific binding on a subsequent tissue section (e.g., a consecutive section on same glass slide) during the same FISH procedure, treated exactly like the specific probes described above.

Protocol

46. Let slides incubate in the dark at room temperature for 20 min.
47. Mount the sections with a fluorophore-compatible antifade mounting medium (e.g., VECTASHIELD) by pipetting a drop onto the tissue and applying a cover slip.
48. Apply gentle pressure on the cover slip to remove all air bubbles. Avoid touching the glass with bare fingers.
    ▲ CRITICAL STEP Avoid air bubbles in the mounting medium when mounting the sections, pockets without mounting medium will bleach quickly under illumination.

Fluorescence microscopy
● TIMING 1 h
49. Acquire an overview image of the sample in bright-field mode (Fig. 4e) and using a fluorescent channel after MALDI–MSI to aid the localization of the analyzed area.
    ◆ TROUBLESHOOTING
50. Compare the overview images acquired before and after MALDI–MSI or FISH to detect potential changes in the tissue integrity (e.g., detached or washed away tissue pieces).
    ▲ CRITICAL STEP If fluorescence dyes are sensitive to bleaching, only acquire a quick overview image using a low-magnification objective lens and short exposure time in the bright-field channel. Alternatively, perform this step after the detail images have been acquired.
51. Acquire fluorescent images of the region measured with MSI in the desired magnification starting with the highest excitation wavelength, proceeding stepwise to higher intensities to reduce bleaching of fluorophores. For *Bathymodiolus* gill sections and probes listed in Table 2, start with the channel for the methanotrophic symbionts (Atto 647), followed by either the thiotrophic symbiont or the intranuclear parasite (Atto 550) and finally the DNA label (DAPI).
    ▲ CRITICAL STEP When selecting the ROI for microscopy, include tissue areas around the region measured with MALDI–MSI (approximately one field of view as a margin around ROI).

Data handling
● TIMING 1 h (computation time is strongly dependent on data size, number of samples and used hardware; time for data analysis also depends heavily on the complexity of the research question)
▲ CRITICAL STEP Many commercially available software tools (e.g., SCiLS Lab Pro and Mirion) allow import of proprietary vendor formats directly; however, we still recommend converting MSI data to the open imzML format[98]. This enables uploading MSI together with the corresponding fluorescence microscopy data to METASPACE (www.metaspace2020.eu) for data sharing. Moreover, metabolite distributions can be browsed on the METASPACE platform. Alternative tools for annotation are MetaboScape (this is currently usable only in combination with initial Bruker MSI data) and LipostarMSI[93]. To infer co-localization of metabolites and cells, a precise overlay of the two imaging modalities is required. This can be done in different ways, but we advise the following step-by-step procedure.
52. First, import the MSI data into suitable analysis software that allows co-registration of optical and MSI data such as Cardinal, Mirion or SCiLS Lab.
53. Generate a combined ion map of three to five abundant metabolites. Commonly, we choose ions with a distribution that outlines the entire measured tissue. Additional guides are the characteristic ions of the applied markings (red pen, observed via m/z 443.2329; white paint, observed via m/z 322.3102 or scratches observed via lack of ions).
54. Process the FISH image and export composite image of DAPI, FISH and marker fluorescent channels, choosing a threshold that illuminates the entire colonized area.
55. Import the FISH image into the MSI analysis software.
56. Start to co-register the FISH image with the MS images; this most likely requires rotation and uniform stretching of the FISH image. Make use of the fiducial marker, which is observable in both modalities (white paint is fluorescent at 640 nm).
    ▲ CRITICAL ROIs can be drawn on the basis of the FISH signals in the microscopy modality to define ROIs in the MALDI modality and typical co-localization analysis can be done to retrieve, e.g., symbiont-specific metabolites. Statistical analysis can be performed comparing, for example, regions defined as bacterially infected versus uninfected tissue.

Protocol

Segmentation can be performed on the MSI data to cluster metabolites based on spatial distribution and identify the metabolites that co-occur with fluorescent signals.

▲ **CRITICAL** Open-source scripts for the implementation of these steps have been published previously and are available via GitHub (R scripts: https://github.com/esogin/miniature-octo-fiesta; MATLAB: https://github.com/BenediktSenorDingDong/MALDI-FISHregistration).

▲ **CRITICAL STEP** Make the overlay of both images as precise as possible. Especially at high spatial resolution, each pixel carries the information of a cell and those have to match with the identity label from FISH. Ablation marks from the MSI laser can be used for precise matching, if they are visible in the optical images.

Troubleshooting

Troubleshooting advice can be found in Table 3.

Table 3 | Troubleshooting table

Step	Problem	Possible reason	Solution
5	Tissue deforms	Tissue too soft	Fill a mold partially with gel, place the sample on top and fill up the mold afterwards
6	CMC block cracks	Freezing too fast	Ensure slow unidirectional freezing from the bottom up by touching only the bottom of the mold to the liquid nitrogen
10	Tissue cannot be localized in CMC block	Pale tissue, low contrast	Dye the embedding medium to increase optical contrast, phenol red can be used, check for mass overlap with metabolites
13	Tissue sections do not adhere	Hard material such as plant tissue	Press down on the section with a flat, sterile surface for a few seconds
		Indium tin oxide coated slides	Manually coat slides with polylysine to allow crosslinking
16	Low contrast in overview image	Wavelength choice	Use blue lasers with an excitation wavelength ~488 nm for the highest animal-tissue autofluorescence. In tissues of plants, cyanobacteria, or algae green lasers with a wavelength of ~510 nm excite chlorophyll and cause red autofluorescence
	Tiled patterns on overview image	Slide scanning microscope settings	Adjust contrast and increase overlap of tiles, alternatively use flatbed scanner for overview images
	Tearing or folded sections	Cryotome settings	See 'Finding the right section thickness'
18	Large crystals or uneven matrix coating	Matrix application parameters	See Box 1
	Tissue and markings not visible	Opaque matrix	Overlay the image recorded in Step 16 to locate the tissue
23	ROI cannot be localized	Low-abundance infection	See 'Finding ROIs for MSI'
26	Paint markings interfere with measurement	Protrusions interfere with laser	Instead of following Step 15, apply scratch marks on tissue with a needle
	Low MSI signal	Laser settings	See Box 2
	Analyte delocalization	Matrix solvents	See Box 1
28	Ablation spots not separated	Step size too small for MSI setup	Treat the data as oversampled or increase pixel size
	Severe tissue damage	Laser intensity too high	Decrease laser intensity, see Box 2
49	Low FISH signal intensity	Tissue damage by MSI	Decrease laser intensity, see Box 2
		Probe choice	See Box 3
	Low DAPI signal intensity	Poor staining	Repeat Step 46 twice with fresh DAPI solution for 10 min
	DAPI signal too bright	Overstaining	Wash slide for 1 min in deionized water

Finding the right section thickness

As a rule of thumb, for high spatial resolution MALDI–MSI (<10 μm) the section thickness should be in the range of the intended lateral resolution of the dataset to keep x, y and z dimensions consistent, 6-μm-thick sections are a good compromise between ease of handling and achievable lateral resolution. If sections rupture or fold in on themselves increase thickness to 10 μm. Signal

Protocol

intensities can be negatively affected by topography introduced by drying or in MALDI-2 setups if the laser can not penetrate. In these cases reduce section thickness.

Cryotome temperatures should be adjusted for different sample types. A higher lipid content (like brain) requires lower temperatures. The chamber temperature should be set 10 °C below sample holder temperature to account for temperature fluctuations when the chamber is opened to manipulate the sample and sections. Very hard samples might require specialized hardware such as tungsten carbide blades[56].

Finding ROIs for MSI

In samples with lowly abundant bacteria and localized infections, it is challenging to locate bacteria on the section for MALDI–MSI. To identify regions with bacteria, we recommend performing FISH on adjacent sections before MSI acquisition to precisely determine the area of measurement. Section 1 is mounted on a glass slide and then FISH is performed as described (Fig. 6). The subsequent section 2 is mounted on a separate glass slide to perform MALDI–MSI. To achieve maximal correlation between FISH and MSI, we advise to flip the consecutive section with a hair of a brush while frozen, so FISH can be performed on the interface shared by both sections. After FISH, overview images of the whole sections are taken with a fluorescence microscope. The areas of infection are marked on the overview image for MALDI, which helps to find the region of infection inside the tissue. Keep in mind that the flipped section is mirrored, which should be considered when searching for the area of infection on the MALDI section.

After matrix application on section 2 for MALDI–MSI, use thin needles or tweezers to mark the area of infection, by carefully setting scratch marks in the matrix/tissue under a stereo-microscope before MALDI–MSI acquisition. After MALDI acquisition, FISH is performed on the same slide to co-localize chemical and taxonomic information, as described. If the tissue section and previous markings are not visible, check the correct position of new markings by overlaying the overview image from Step 16 to compare.

Timing

Steps 1–13, cryoembedding and cryosectioning: 2–3 h (depending on experience level and number of sections cut)
Steps 14–16, marking and microscopy: 30 min
Steps 17–19, matrix application: 1 h
Steps 20–27, MSI: 30 min setup + measurement time (Table 1, hours to days for very large measurement areas)
Step 28, overview image: 30 min
Steps 29–32, fixation of samples after MSI: 2–3 h
Steps 33–48, FISH: ~3 h
Steps 49–51, fluorescence microscopy: 1 h
Steps 52–56, data handling: 1 h (computation time is dependent on data size, number of samples and available hardware; time for data analysis depends on the complexity of research question)

Anticipated results

The presented metaFISH protocol allows simultaneous mapping of metabolites and bacteria in a single tissue section. After successful implementation, a dataset will comprise several hundred metabolite maps and fluorescence microscopy images showing the distribution of bacterial cells in the tissue. A typical result is shown in Fig. 7, where cross-sections through an earthworm reveal a hotspot of an unknown metabolite (m/z 1,116.833 ± 0.224 Da), which colocalizes with the FISH signal of symbiotic bacteria. In total, five ion species were clearly co-localized with the FISH signal, none of which could be identified as a known metabolite on the basis of database matching[40].

Protocol

We further illustrated the compatibility of metaFISH with several different FISH probes on one sample using a deep-sea mussel symbiosis. Here, bacterial symbionts are each labeled with a unique fluorescent probe, detecting specific and unique 16S rRNA sequences. Metabolite
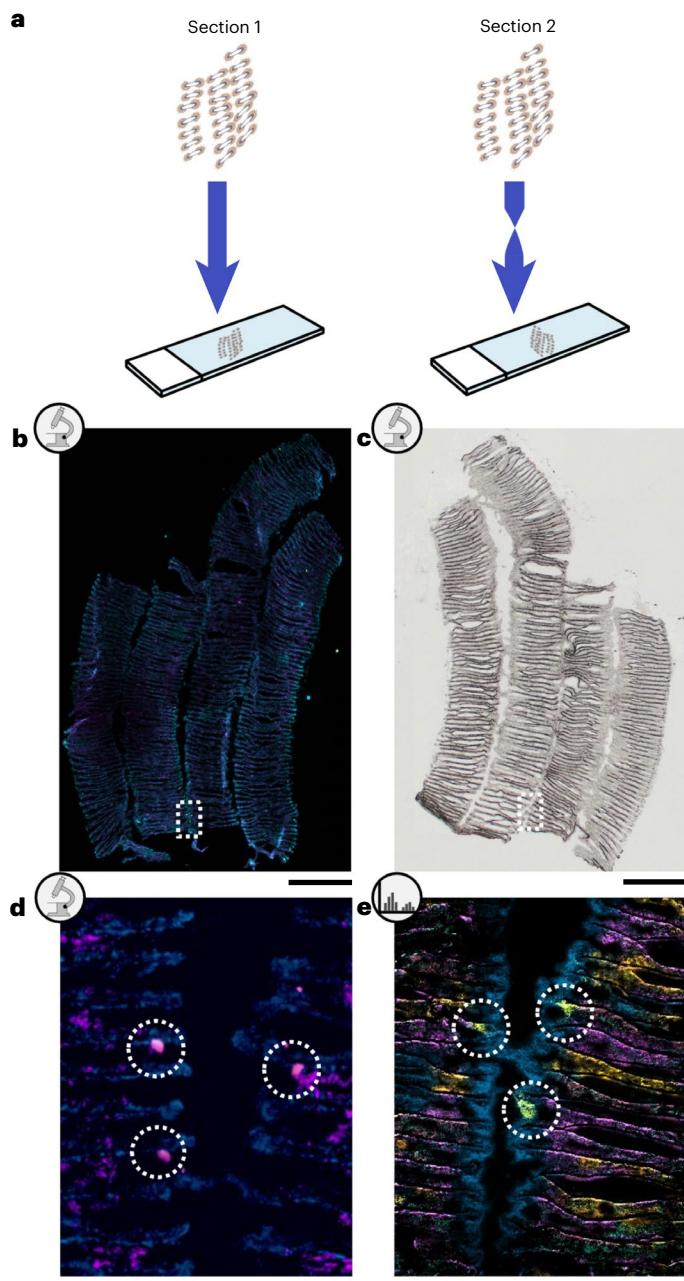

Fig. 6 | Identifying bacterial infection sites for high-resolution MALDI–MSI. Identifying the site of bacterial infection in the host tissue before conducting high-resolution MALDI–MSI is critical to reduce measurement times. **a**, To screen for bacterial infections in the tissue in *Bathymodiolus childressi* gill sections, we use an alternating approach of FISH (section 1) and MALDI–MSI (section 2). To ensure precise correlations, section 2 is flipped. This ensures that adjacent sectioning planes are both facing upwards when mounted on the glass slides. **b**, First, FISH is performed on section 1 to identify bacteria in the tissue based on their fluorescent signal. **c**, The corresponding region is marked on the flipped section 2 for MSI. **d**, Zoom-in of **b**, ROI selection based on FISH image showing three individual infected host cells (dashed circles). **e**, MALDI–MSI of the corresponding ROI on adjacent tissue section showing a metabolite detected in infected cells (dashed circles, yellow, *m/z* 716.5216 ± 5 ppm). MSI data were recorded with a prototype t-MALDI-2 setup[21] at 2 μm pixel size; DHAP matrix was applied by sublimation. Scale bars: **b** and **c**, 2 mm; **d** and **e**, 100 μm.
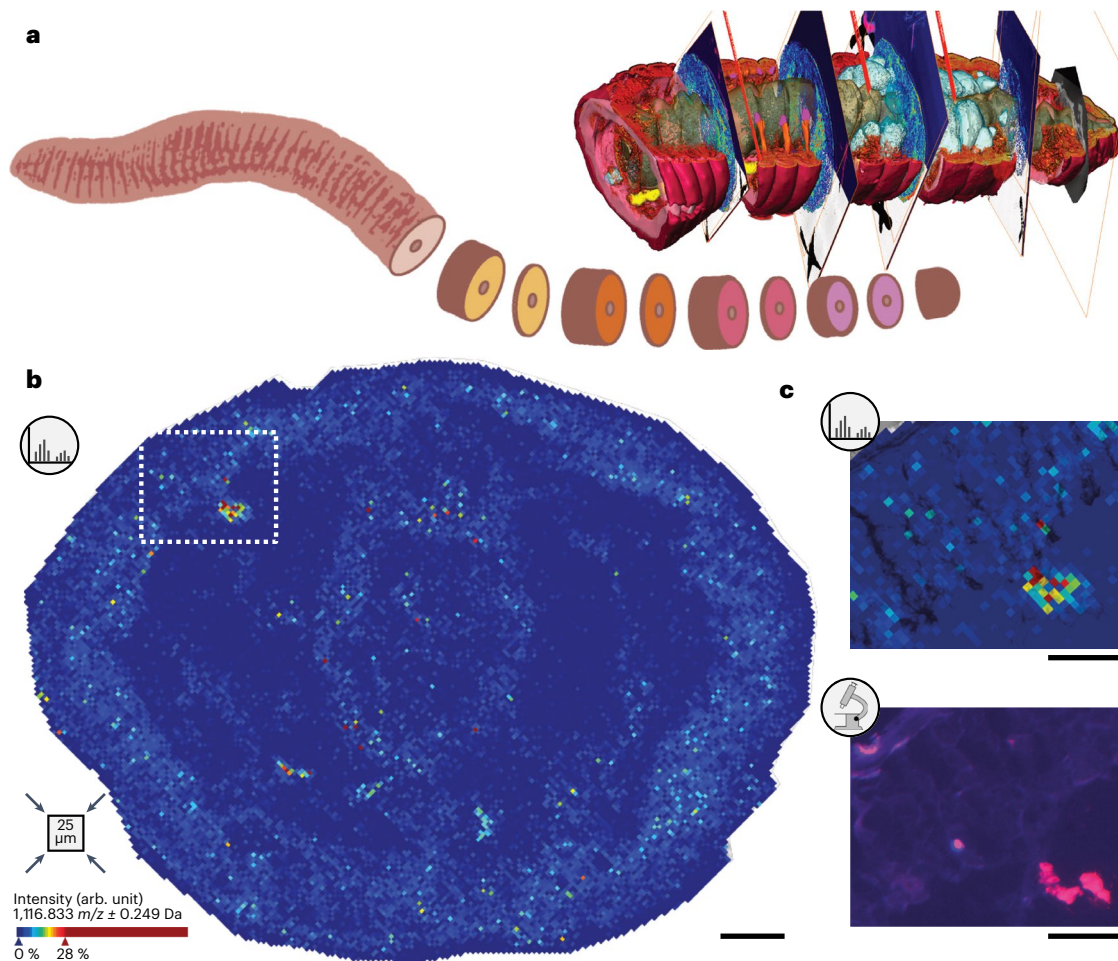
Fig. 7 | Metabolites co-localize with a patch of bacterial cells in earthworm tissue. a, Schematic of the animal and the used sectioning planes. **b**, MALDI–MSI (Autoflex speed LRF MALDI-TOF, pixel size 25 μm, matrix α-cyano-4-hydroxycinnamic acid (CHCA) applied with spraying) ion image of unidentified metabolite with *m/z* 1,116.833 ± 0.224 Da showing the highest co-localization value with FISH signals for symbiotic bacteria. White dashed line outlines the magnified region in **c. c**, Top: zoom-in on a metabolite hotspot; bottom: the corresponding FISH microscopy image. Scale bars, **b**, 500 μm; **c**, 250 μm. Panels **a**–**c** adapted from ref. 40, PNAS.

distributions were co-localized with symbiotic bacteria, parasitic bacteria or uncolonized host tissue. MSI ion maps are shown for metabolites at different spatial resolutions in combination with the microscopy. This comparison on similar animals shows how pixel size can influence the results of metaFISH. The smallest published pixel size for MALDI–MSI data correlated with FISH of 3 μm in Fig. 8e demonstrates the visual separation of colonized host cells (bacteriocytes). This dataset revealed metabolite differences (e.g., bacteriohopanoids) between bacteriocytes colonized with similar symbionts (based on the microscopy data with a specific 16S rRNA probe). The bigger pixel size of 10 μm shows the presence of specific localized metabolites (e.g., not annotated *m*/z 890.4951, see Fig. 8c), which matches the FISH signal of parasitic bacteria in the ciliated edge of the mussel gill tissue. This metabolite could be a product of the bacterium or could indicate a response of the mussel host towards the infection. For the here-presented spatial metabolomics examples of gills from *Bathymodiolus* mussels, we commonly observed above 5,000 peaks, of which usually between 100 and 500 are putatively annotated (false discovery rate, 20%) by www.metaspace2020.eu (Supplementary Information). This relatively low metabolite identification rate is also common for other metabolomics experiments[78].
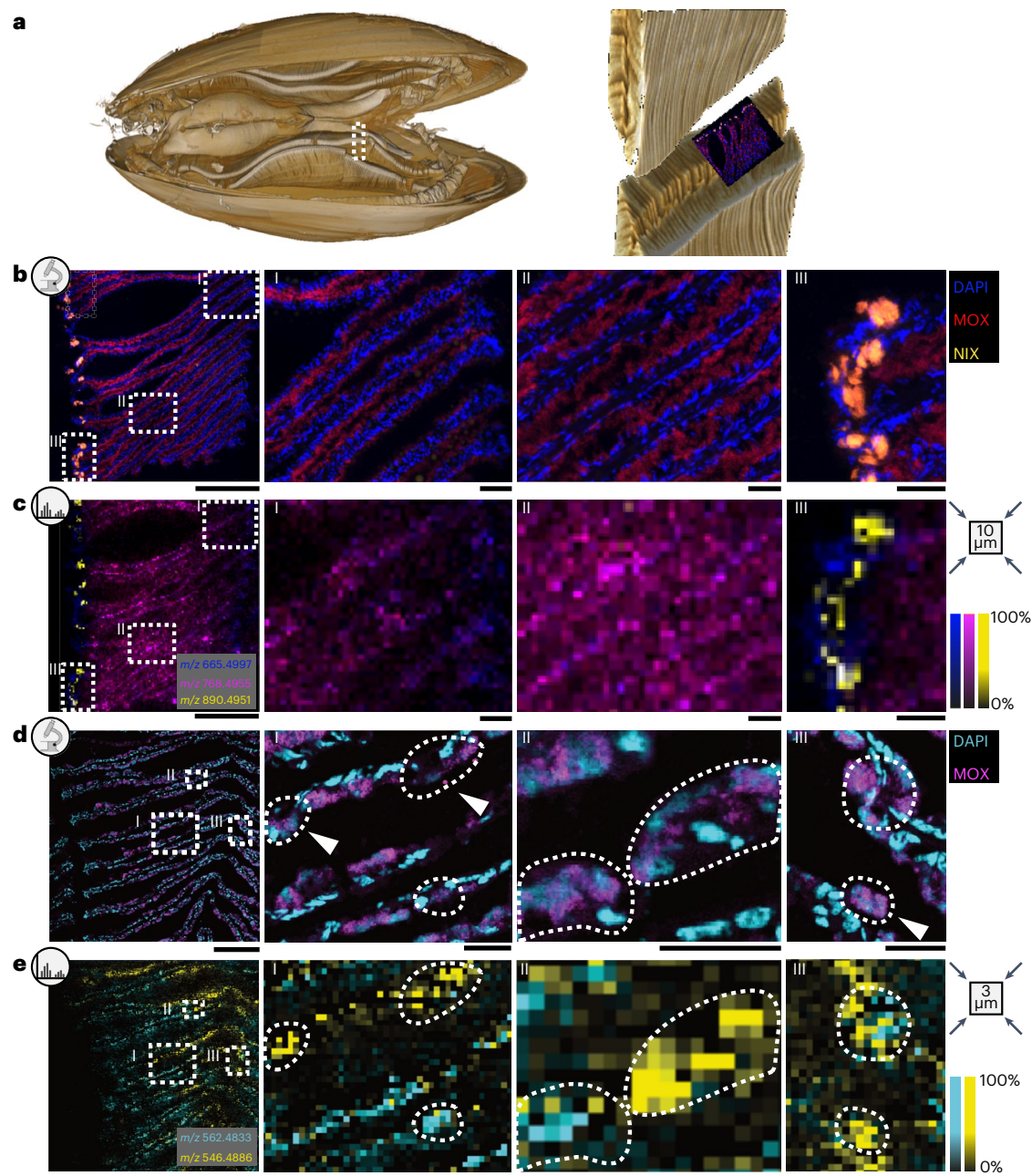
Fig. 8 | metaFISH reveals metabolite distributions correlated with the presence of symbionts and parasites at 10 μm and 3 μm resolution.
a, Microcomputed tomography and three-dimensional reconstruction of whole *Bathymodiolus* mussel. On the right, a virtual dissection of the gill and horizontal sectioning plane through gill filaments indicating area covered below. **b**–**e**, Regions analyzed with MALDI–MSI and FISH with three regions (I–III) magnified. **b**, FISH image of *Bathymodiolus childressi* infected with an intranuclear parasite. Microscopy channels: red, EUB I general bacteria probe (majority of signals from the methanotrophic symbiont (MOX); yellow: specific probe for parasitic bacterium, nuclear inclusion factor X (NIX) (based on ref.103); blue: DAPI as general DNA stain. **c**, MALDI–MSI (AP-SMALDI-5 AF, 10 μm pixel size, sDHB matrix applied by spraying) ion maps of the regions shown in **b**, magenta: *m/z* 768.4955 ± 5 ppm, yellow: *m/z* 890.4951 ± 5 ppm, blue: *m/z* 665.4997 ± 5 ppm, pixel size 10 μm. Scale bars: overview, 200 μm; magnified regions, 100 μm. **d**, FISH image of *Bathymodiolus puteoserpentis* gill section, magenta: specific probe for methanotrophic symbionts (MOX); cyan: DAPI general DNA stain. Scale bars: overview, 150 μm; magnified regions, 50 μm. **e**, MALDI–MSI (AP-SMALDI prototype with advanced optics[22], pixels size 3 μm, matrix sDHB applied by spraying) overlay of ion maps: cyan: bacteriohopane-32,33,34,35-tetrol; *m/z* 562.4883, here shown [M+H]+ ion *m/z* = 563.4670 ± 5 ppm, yellow: 35-aminobacteriohopane-31,32,33,34-tetrol; *m/z* 546.4886, here shown [M+H]+ ion *m/z* 547.4720 ± 5 ppm. Scale bars: overview images in left column, 150 μm; magnified regions in columns 2–4, 50 μm. Dashed outlines in magnified regions of **d** and **e** mark individual bacteriocytes, white arrowheads indicate bacteriocytes in which only 35-aminobacteriohopane-31,32,33,34-tetrol was detected. Scale bars: overview, 200 μm; magnified regions, 100 μm. Panels **a**, **d** and **e** adapted from ref. 6, Springer Nature Limited.

Protocol

For metabolites with relevant distributions for host–microbe interactions, which are not annotated by any database search, typically steps for structure elucidation need to follow. This includes on-tissue MS^2 and further MS^2 experiments with extracts of tissues via LC–MS^2 as we have shown for a group of metabolites in the *Bathymodiolus* symbiosis[6]. For full structure confirmation of newly identified metabolites, additional experiments with complementary methods such as NMR are needed[99].

In summary, the here-presented applications of metaFISH provide an insight into the functional and chemical ecology of host–microbe interactions on a metabolite level and at high spatial resolution. The rapid and continuous advancements of the MALDI–MSI technology enables microbiologists to image microbial colonies, biofilms and single eukaryotic cells and even bacterial microcolonies. Today, MALDI–MSI is at the cusp of resolving single bacterial cells. The here-presented metaFISH protocol provides the groundwork for analyzing and understanding these micrometer-scale bacterial metabolomes.

Data availability

All data presented in this paper have been deposited in the METASPACE project protocol (https://metaspace2020.eu/project/metaFISH). Individual datasets are deposited as follows: Fig. 1, MPIMM_193_QE_P_BC_CF (https://metaspace2020.eu/dataset/2019-11-28_11h08m15s); Fig. 5, 20210518_b_child_nix_s1_dhap_maldi2_tof_5um_laser90%_50shots (https://metaspace2020.eu/dataset/2021-07-08_13h54m26s), 20210518_b_child_nix_s1_dhap_laser70%_shots50 (https://metaspace2020.eu/dataset/2021-05-30_18h51m15s), 20210518_b_child_nix_s1_dhap_5um_maldi2_tof_laser50%_100 (https://metaspace2020.eu/dataset/2021-05-30_18h08m20s), 20210518_b_child_nix_s1_dhap_5um_maldi2_tof_laser30%_150 (https://metaspace2020.eu/dataset/2021-05-30_18h08m14s), and MPIMM_299_TTF_M2_Grid (https://metaspace2020.eu/dataset/2023-01-26_10h37m44s); Fig. 6, 20210706_bchild_nix_n25_tm_sl108 (https://metaspace2020.eu/dataset/2021-07-08_15h03m30s); Fig. 7, MTBLS2639; and Fig. 8, MPIMM_054_QE_P_BP_CF (https://metaspace2020.eu/dataset/2017-03-28_16h40m57s) and MPIMM_193_QE_P_BC_CF (https://metaspace2020.eu/dataset/2019-11-28_11h08m15s).

Code availability

Open-source scripts for the implementation of the MSI and microscopy co-registration have been published previously[6] and are available on GitHub (R scripts, https://github.com/esogin/miniature-octo-fiesta; MATLAB, https://github.com/BenediktSenorDingDong/MALDI-FISHregistration).

References

1. Moses, L. & Pachter, L. Museum of spatial transcriptomics. *Nat. Methods* **19**, 534–546 (2022).
2. Mund, A., Brunner, A.-D. & Mann, M. Unbiased spatial proteomics with single-cell resolution in tissues. *Mol. Cell* **82**, 2335–2349 (2022).
3. Bauermeister, A., Mannochio-Russo, H., Costa-Lotufo, L. V., Jarmusch, A. K. & Dorrestein, P. C. Mass spectrometry-based metabolomics in microbiome investigations. *Nat. Rev. Microbiol.* **20**, 143–160 (2022).
4. Wishart, D. S. et al. NMR and metabolomics—a roadmap for the future. *Metabolites* **12**, 678 (2022).
5. Alexandrov, T. Spatial metabolomics and imaging mass spectrometry in the age of artificial intelligence. *Annu. Rev. Biomed. Data Sci.* **3**, 61–87 (2020).
6. Geier, B. et al. Spatial metabolomics of in situ host–microbe interactions at the micrometre scale. *Nat. Microbiol.* **5**, 498–510 (2020).
7. Esquenazi, E., Yang, Y.-L., Watrous, J., Gerwick, W. H. & Dorrestein, P. C. Imaging mass spectrometry of natural products. *Nat. Prod. Rep.* **26**, 1521–1534 (2009).
8. Vickerman, J. C. Molecular imaging and depth profiling by mass spectrometry—SIMS, MALDI or DESI. *Analyst* **136**, 2199–2217 (2011).
9. Pozebon, D., Scheffler, G. L., Dressler, V. L. & Nunes, M. A. G. Review of the applications of laser ablation inductively coupled plasma mass spectrometry (LA-ICP-MS) to the analysis of biological samples. *J. Anal. At. Spectrom.* **29**, 2204–2228 (2014).
10. Heijs, B., Potthoff, A., Soltwisch, J. & Dreisewerd, K. MALDI-2 for the enhanced analysis of N-linked glycans by mass spectrometry imaging. *Anal. Chem.* **92**, 13904–13911 (2020).
11. Stanback, A. E. et al. Regional *N*-glycan and lipid analysis from tissues using MALDI–mass spectrometry imaging. *STAR Protoc.* **2**, 100304 (2021).
12. Sun, C. et al. Visualizing the spatial distribution and alteration of metabolites in continuously cropped *Salvia miltiorrhiza* Bge using MALDI–MSI. *J. Pharm. Anal.* **12**, 719–724 (2022).
13. Sogin, E. M. et al. Sugars dominate the seagrass rhizosphere. *Nat. Ecol. Evol.* **6**, 866–877 (2022).

Protocol

14. Bien, T., Koerfer, K., Schwenzfeier, J., Dreisewerd, K. & Soltwisch, J. Mass spectrometry imaging to explore molecular heterogeneity in cell culture. *Proc. Natl Acad. Sci. USA* **119**, e2114365119 (2022).

15. Capolupo, L. et al. Sphingolipids control dermal fibroblast heterogeneity. *Science* **376**, eabh1623 (2022).

16. Bourceau, P., Michellod, D., Geier, B. & Liebeke, M. Spatial metabolomics shows contrasting phosphonolipid distributions in tissues of marine bivalves. *PeerJ Anal. Chem.* **4**, e21 (2022).

17. Bowman, A. P. et al. Evaluation of lipid coverage and high spatial resolution MALDI-imaging capabilities of oversampling combined with laser post-ionisation. *Anal. Bioanal. Chem.* **412**, 2277–2289 (2020).

18. Rappez, L. et al. SpaceM reveals metabolic states of single cells. *Nat. Methods* **18**, 799–805 (2021).

19. Wang, G. et al. Analyzing cell-type-specific dynamics of metabolism in kidney repair. *Nat. Metab.* **4**, 1109–1118 (2022).

20. Zhu, X., Xu, T., Peng, C. & Wu, S. Advances in MALDI mass spectrometry imaging single cell and tissues. *Front. Chem.* **9**, 782432 (2022).

21. Niehaus, M., Soltwisch, J., Belov, M. E. & Dreisewerd, K. Transmission-mode MALDI-2 mass spectrometry imaging of cells and tissues at subcellular resolution. *Nat. Methods* **16**, 925–931 (2019).

22. Kompauer, M., Heiles, S. & Spengler, B. Atmospheric pressure MALDI mass spectrometry imaging of tissues and cells at 1.4-µm lateral resolution. *Nat. Methods* **14**, 90–96 (2017).

23. Yang, J. Y. et al. Primer on agar-based microbial imaging mass spectrometry. *J. Bacteriol.* **194**, 6023–6028 (2012).

24. Yang, Y.-L., Xu, Y., Straight, P. & Dorrestein, P. C. Translating metabolic exchange with imaging mass spectrometry. *Nat. Chem. Biol.* **5**, 885–887 (2009).

25. Si, T. et al. Characterization of *Bacillus subtilis* colony biofilms via mass spectrometry and fluorescence imaging. *J. Proteome Res.* **15**, 1955–1962 (2016).

26. Feucherolles, M. & Frache, G. MALDI mass spectrometry imaging: a potential game-changer in a modern microbiology. *Cells* **11**, 3900 (2022).

27. Dunham, S. J. B., Ellis, J. F., Li, B. & Sweedler, J. V. Mass spectrometry imaging of complex microbial communities. *Acc. Chem. Res.* **50**, 96–104 (2017).

28. Gahlmann, A. & Moerner, W. E. Exploring bacterial cell biology with single-molecule tracking and super-resolution imaging. *Nat. Rev. Microbiol.* **12**, 9–22 (2014).

29. Hatzenpichler, R., Krukenberg, V., Spietz, R. L. & Jay, Z. J. Next-generation physiology approaches to study microbiome function at single cell level. *Nat. Rev. Microbiol.* **18**, 241–256 (2020).

30. Amann, R. & Fuchs, B. M. Single-cell identification in microbial communities by improved fluorescence in situ hybridization techniques. *Nat. Rev. Microbiol.* **6**, 339–348 (2008).

31. Amann, R., Fuchs, B. M. & Behrens, S. The identification of microorganisms by fluorescence in situ hybridisation. *Curr. Opin. Biotechnol.* **12**, 231–236 (2001).

32. Barrero-Canosa, J., Moraru, C., Zeugner, L., Fuchs, B. M. & Amann, R. Direct-geneFISH: a simplified protocol for the simultaneous detection and quantification of genes and rRNA in microorganisms. *Environ. Microbiol.* **19**, 70–82 (2017).

33. Greuter, D., Loy, A., Horn, M. & Rattei, T. probeBase—an online resource for rRNA-targeted oligonucleotide probes and primers: new features 2016. *Nucleic Acids Res.* **44**, D586–D589 (2015).

34. Smith, B. et al. Community analysis of bacteria colonizing intestinal tissue of neonates with necrotizing enterocolitis. *BMC Microbiol.* **11**, 73 (2011).

35. Schimak, M. P., Toenshoff, E. R. & Bright, M. Simultaneous 16S and 18S rRNA fluorescence in situ hybridization (FISH) on LR White sections demonstrated in Vestimentifera (Siboglinidae) tubeworms. *Acta Histochem.* **114**, 122–130 (2012).

36. Neugent, M. L., Gadhvi, J., Palmer, K. L., Zimmern, P. E. & De Nisco, N. J. Detection of tissue-resident bacteria in bladder biopsies by 16S rRNA fluorescence in situ hybridization. *J Vis. Exp.* **152**, e60458 (2019).

37. Valm, A. M., Mark Welch, J. L. & Borisy, G. G. CLASI-FISH: principles of combinatorial labeling and spectral imaging. *Syst. Appl. Microbiol.* **35**, 496–502 (2012).

38. Valm, A. M. et al. Systems-level analysis of microbial community organization through combinatorial labeling and spectral imaging. *Proc. Natl Acad. Sci. USA* **108**, 4152–4157 (2011).

39. Kaltenpoth, M., Strupat, K. & Svatoš, A. Linking metabolite production to taxonomic identity in environmental samples by (MA)LDI-FISH. *ISME J.* **10**, 527–531 (2016).

40. Geier, B. et al. Connecting structure and function from organisms to molecules in small-animal symbioses through chemo-histo-tomography. *Proc. Natl Acad. Sci. USA* **118**, e2023773118 (2021).

41. Ponnudurai, R. et al. Metabolic and physiological interdependencies in the *Bathymodiolus azoricus* symbiosis. *ISME J.* **11**, 463–477 (2017).

42. Dreisewerd, K., Bien, T. & Soltwisch, J. in *Mass Spectrometry Imaging of Small Molecules: Methods and Protocols* (ed. Y.-J. Lee) 21–40 (Springer, 2022).

43. Soltwisch, J. et al. Mass spectrometry imaging with laser-induced postionization. *Science* **348**, 211–215 (2015).

44. Ansorge, R. et al. Functional diversity enables multiple symbiont strains to coexist in deep-sea mussels. *Nat. Microbiol.* **4**, 2487–2497 (2019).

45. Fung, C. et al. High-resolution mapping reveals that microniches in the gastric glands control *Helicobacter pylori* colonization of the stomach. *PLoS Biol.* **17**, e3000231 (2019).

46. Lackner, G., Peters, E. E., Helfrich, E. J. N. & Piel, J. Insights into the lifestyle of uncultured bacterial natural product factories associated with marine sponges. *Proc. Natl Acad. Sci. USA* **114**, E347–E356 (2017).

47. Yang, H. et al. On-tissue derivatization of lipopolysaccharide for detection of Lipid A using MALDI-MSI. *Anal. Chem.* **92**, 13667–13671 (2020).

48. Patel, E. et al. MALDI-MS imaging for the study of tissue pharmacodynamics and toxicodynamics. *Bioanalysis* **7**, 91–101 (2015).

49. Prideaux, B. et al. High-sensitivity MALDI–MRM–MS imaging of moxifloxacin distribution in tuberculosis-infected rabbit lungs and granulomatous lesions. *Anal. Chem.* **83**, 2112–2118 (2011).

50. Daims, H., Brühl, A., Amann, R., Schleifer, K.-H. & Wagner, M. The domain-specific probe EUB338 is insufficient for the detection of all bacteria: development and evaluation of a more comprehensive probe set. *Syst. Appl. Microbiol.* **22**, 434–444 (1999).

51. Braun, P. et al. In-depth analysis of *Bacillus anthracis* 16S rRNA genes and transcripts reveals intra- and intergenomic diversity and facilitates anthrax detection. *mSystems* **7**, e01361–01321 (2022).

52. Rath, C. M. et al. Molecular analysis of model gut microbiotas by imaging mass spectrometry and nanodesorption electrospray ionization reveals dietary metabolite transformations. *Anal. Chem.* **84**, 9259–9267 (2012).

53. Piwosz, K., Mukherjee, I., Salcher, M. M., Grujčić, V. & Šimek, K. CARD-FISH in the sequencing era: opening a new universe of protistan ecology. *Front. Microbiol.* **12**, 640066 (2021).

54. Morales, D. P. et al. Advances and challenges in fluorescence in situ hybridization for visualizing fungal endobacteria. *Front. Microbiol.* **13**, 892227 (2022).

55. Raj, A., van den Bogaard, P., Rifkin, S. A., van Oudenaarden, A. & Tyagi, S. Imaging individual mRNA molecules using multiple singly labeled probes. *Nat. Methods* **5**, 877–879 (2008).

56. Ticha, P. et al. A novel cryo-embedding method for in-depth analysis of craniofacial mini pig bone specimens. *Sci. Rep.* **10**, 19510 (2020).

57. Hoffmann, F., Janussen, D., Dröse, W., Arp, G. & Reitner, J. Histological investigation of organisms with hard skeletons: a case study of siliceous sponges. *Biotech. Histochem.* **78**, 191–199 (2003).

58. Kompauer, M., Heiles, S. & Spengler, B. Autofocusing MALDI mass spectrometry imaging of tissue sections and 3D chemical topography of nonflat surfaces. *Nat. Methods* **14**, 1156–1158 (2017).

59. Angerer, T. B., Bour, J., Biagi, J.-L., Moskovets, E. & Frache, G. Evaluation of 6 MALDI–matrices for 10 µm lipid imaging and on-tissue MSn with AP-MALDI-Orbitrap. *J. Am. Soc. Mass Spectrom.* **33**, 760–771 (2022).

60. Leopold, J., Prabutzki, P., Engel, K. M. & Schiller, J. A five-year update on matrix compounds for MALDI–MS analysis of lipids. *Biomolecules* **13**, 546 (2023).

61. Cerruti, C. D., Benabdellah, F., Laprévote, O., Touboul, D. & Brunelle, A. MALDI imaging and structural analysis of rat brain lipid negative ions with 9-aminoacridine matrix. *Anal. Chem.* **84**, 2164–2171 (2012).

62. Kaya, I., Jennische, E., Lange, S. & Malmberg, P. Dual polarity MALDI imaging mass spectrometry on the same pixel points reveals spatial lipid localizations at high-spatial resolutions in rat small intestine. *Anal. Methods* **10**, 2428–2435 (2018).

63. Meisenbichler, C., Doppler, C., Bernhard, D. & Müller, T. Improved matrix coating for positive- and negative-ion-mode MALDI-TOF imaging of lipids in blood vessel tissues. *Anal. Bioanal. Chem.* **411**, 3221–3227 (2019).

64. Shariatgorji, R. et al. Spatial visualization of comprehensive brain neurotransmitter systems and neuroactive substances by selective in situ chemical derivatization mass spectrometry imaging. *Nat. Protoc.* **16**, 3298–3321 (2021).

65. Iwama, T. et al. Development of an on-tissue derivatization method for MALDI mass spectrometry imaging of bioactive lipids containing phosphate monoester using Phos-tag. *Anal. Chem.* **93**, 3867–3875 (2021).

66. Harkin, C. et al. On-tissue chemical derivatization in mass spectrometry imaging. *Mass Spectrom. Rev.* **41**, 662–694 (2022).

67. Tressler, C. et al. Factorial design to optimize matrix spraying parameters for MALDI mass spectrometry imaging. *J. Am. Soc. Mass Spectrom.* **32**, 2728–2737 (2021).

68. Ščupáková, K. et al. Cellular resolution in clinical MALDI mass spectrometry imaging: the latest advancements and current challenges. *Clin. Chem. Lab. Med.* **58**, 914–929 (2020).

69. Schimak, M. P. et al. MiL-FISH: multilabeled oligonucleotides for fluorescence in situ hybridization improve visualization of bacterial cells. *Appl. Environ. Microbiol.* **82**, 62–70 (2016).

70. Amann, R. I., Krumholz, L. & Stahl, D. A. Fluorescent-oligonucleotide probing of whole cells for determinative, phylogenetic, and environmental studies in microbiology. *J. Bacteriol.* **172**, 762–770 (1990).

71. Folberth, J., Begemann, K., Jöhren, O., Schwaninger, M. & Othman, A. MS(2) and LC libraries for untargeted metabolomics: Enhancing method development and identification confidence. *J. Chromatogr. B* **1145**, 122105 (2020).

72. Chaleckis, R., Meister, I., Zhang, P. & Wheelock, C. E. Challenges, progress and promises of metabolite annotation for LC–MS-based metabolomics. *Curr. Opin. Biotechnol.* **55**, 44–50 (2019).

73. Palmer, A. et al. FDR-controlled metabolite annotation for high-resolution imaging mass spectrometry. *Nat. Methods* **14**, 57–60 (2017).

74. Spraggins, J. M. et al. High-performance molecular imaging with MALDI trapped ion-mobility time-of-flight (timsTOF) mass spectrometry. *Anal. Chem.* **91**, 14552–14560 (2019).

75. Kim, Y. H. et al. In situ label-free visualization of orally dosed strictinin within mouse kidney by MALDI–MS imaging. *J. Agric. Food Chem.* **62**, 9279–9285 (2014).

Protocol

76. Pirman, D. A., Reich, R. F., Kiss, A. A., Heeren, R. M. A. & Yost, R. A. Quantitative MALDI tandem mass spectrometric imaging of cocaine from brain tissue with a deuterated internal standard. *Anal. Chem.* **85**, 1081–1089 (2013).

77. Amann, R. I., Ludwig, W. & Schleifer, K. H. Phylogenetic identification and in situ detection of individual microbial cells without cultivation. *Microbiol. Rev.* **59**, 143–169 (1995).

78. Janda, M. et al. Determination of abundant metabolite matrix adducts illuminates the dark metabolome of MALDI-mass spectrometry imaging datasets. *Anal. Chem.* **93**, 8399–8407 (2021).

79. Protsyuk, I. et al. 3D molecular cartography using LC–MS facilitated by Optimus and 'ili software. *Nat. Protoc.* **13**, 134–154 (2018).

80. Garg, N. et al. Three-dimensional microbiome and metabolome cartography of a diseased human lung. *Cell Host Microbe* **22**, 705–716.e704 (2017).

81. Shen, S. et al. Parallel, high-quality proteomic and targeted metabolomic quantification using laser capture microdissected tissues. *Anal. Chem.* **93**, 8711–8718 (2021).

82. Dilillo, M. et al. Mass spectrometry imaging, laser capture microdissection, and LC–MS/MS of the same tissue section. *J. Proteome Res.* **16**, 2993–3001 (2017).

83. Ščupáková, K., Dewez, F., Walch, A. K., Heeren, R. M. A. & Balluff, B. Morphometric cell classification for single-cell MALDI–mass spectrometry imaging. *Angew. Chem. Int. Ed.* **59**, 17447–17450 (2020).

84. Prade, V. M. et al. De novo discovery of metabolic heterogeneity with immunophenotype-guided imaging mass spectrometry. *Mol. Metabol.* **36**, 100953 (2020).

85. Blanc, L., Lenaerts, A., Dartois, V. & Prideaux, B. Visualization of mycobacterial biomarkers and tuberculosis drugs in infected tissue by MALDI–MS imaging. *Anal. Chem.* **90**, 6275–6282 (2018).

86. Perry, W. J. et al. *Staphylococcus aureus* exhibits heterogeneous siderophore production within the vertebrate host. *Proc. Natl Acad. Sci. USA* **116**, 21980–21982 (2019).

87. Tobias, F. & Hummon, A. B. Considerations for MALDI-based quantitative mass spectrometry imaging studies. *J. Proteome Res.* **19**, 3620–3630 (2020).

88. Bakker, B. et al. Preparing ductal epithelial organoids for high-spatial-resolution molecular profiling using mass spectrometry imaging. *Nat. Protoc.* **17**, 962–979 (2022).

89. Paschke, C. et al. Mirion—a software package for automatic processing of mass spectrometric images. *J. Am. Soc. Mass Spectrom.* **24**, 1296–1306 (2013).

90. Bemis, K. D. et al. Cardinal: an R package for statistical analysis of mass spectrometry-based imaging experiments. *Bioinformatics* **31**, 2418–2420 (2015).

91. Race, A. M., Styles, I. B. & Bunch, J. Inclusive sharing of mass spectrometry imaging data requires a converter for all. *J. Proteomics* **75**, 5111–5112 (2012).

92. Goracci, L. et al. Lipostar, a comprehensive platform-neutral cheminformatics tool for lipidomics. *Anal. Chem.* **89**, 6257–6264 (2017).

93. Tortorella, S. et al. LipostarMSI: comprehensive, vendor-neutral software for visualization, data analysis, and automated molecular identification in mass spectrometry imaging. *J. Am. Soc. Mass Spectrom.* **31**, 155–163 (2020).

94. Treu, A. & Römpp, A. Matrix ions as internal standard for high mass accuracy matrix-assisted laser desorption/ionization mass spectrometry imaging. *Rapid Commun. Mass Spectrom.* **35**, e9110 (2021).

95. Sládková, K., Houška, J. & Havel, J. Laser desorption ionization of red phosphorus clusters and their use for mass calibration in time-of-flight mass spectrometry. *Rapid Commun. Mass Spectrom.* **23**, 3114–3118 (2009).

96. He, J., Mo, D., Chen, J. & Luo, L. Combined whole-mount fluorescence in situ hybridization and antibody staining in zebrafish embryos and larvae. *Nat. Protoc.* **15**, 3361–3379 (2020).

97. Richardson, D. S. et al. Tissue clearing. *Nat. Rev. Methods Primers* **1**, 84 (2021).

98. Schramm, T. et al. imzML—a common data format for the flexible exchange and processing of mass spectrometry imaging data. *J. Proteomics* **75**, 5106–5110 (2012).

99. Sumner, L. W. et al. Proposed minimum reporting standards for chemical analysis Chemical Analysis Working Group (CAWG) Metabolomics Standards Initiative (MSI). *Metabolomics* **3**, 211–221 (2007).

100. Bik, L. et al. In vivo dermal delivery of bleomycin with electronic pneumatic injection: drug visualization and quantification with mass spectrometry. *Expert Opin. Drug Deliv.* **19**, 213–219 (2022).

101. Cuypers, E. et al. 'On the spot' digital pathology of breast cancer based on single-cell mass spectrometry imaging. *Anal. Chem.* **94**, 6180–6190 (2022).

102. Duperron, S. et al. A dual symbiosis shared by two mussel species, *Bathymodiolus azoricus* and *Bathymodiolus puteoserpentis* (Bivalvia: Mytilidae), from hydrothermal vents along the northern Mid-Atlantic Ridge. *Environ. Microbiol.* **8**, 1441–1447 (2006).

103. Zielinski, F. U. et al. Widespread occurrence of an intranuclear bacterial parasite in vent and seep bathymodiolin mussels. *Environ. Microbiol.* **11**, 1150–1167 (2009).

104. Raskin, L., Stromley, J. M., Rittmann, B. E. & Stahl, D. A. Group-specific 16S rRNA hybridization probes to describe natural communities of methanogens. *Appl. Environ. Microbiol.* **60**, 1232–1240 (1994).

105. Manz, W., Amann, R., Ludwig, W., Wagner, M. & Schleifer, K.-H. Phylogenetic oligodeoxynucleotide probes for the major subclasses of proteobacteria: problems and solutions. *Syst. Appl. Microbiol.* **15**, 593–600 (1992).

106. Hayasaka, T., Goto-Inoue, N., Masaki, N., Ikegami, K. & Setou, M. Application of 2,5-dihydroxyacetophenone with sublimation provides efficient ionization of lipid species by atmospheric pressure matrix-assisted laser desorption/ionization imaging mass spectrometry. *Surf. Interface Anal.* **46**, 1219–1222 (2014).

107. Bien, T., Hambleton, E. A., Dreisewerd, K. & Soltwisch, J. Molecular insights into symbiosis—mapping sterols in a marine flatworm-algae-system using high spatial resolution MALDI-2-MS imaging with ion mobility separation. *Anal. Bioanal. Chem.* **413**, 2767–2777 (2021).

108. Ellis, S. R., Soltwisch, J., Paine, M. R. L., Dreisewerd, K. & Heeren, R. M. A. Laser post-ionisation combined with a high resolving power orbitrap mass spectrometer for enhanced MALDI–MS imaging of lipids. *Chem. Commun.* **53**, 7246–7249 (2017).

109. Zhou, Q. et al. A caged in-source laser-cleavable MALDI matrix with high vacuum stability for extended MALDI–MS imaging. *Angew. Chem. Int. Ed.* **62**, e202217047 (2023).

110. Lukowski, J. K. et al. Storage conditions of human kidney tissue sections affect spatial lipidomics analysis reproducibility. *J. Am. Soc. Mass Spectrom.* **31**, 2538–2546 (2020).

111. Stoecker, K., Dorninger, C., Daims, H. & Wagner, M. Double labeling of oligonucleotide probes for fluorescence in situ hybridization (DOPE-FISH) improves signal intensity and increases rRNA accessibility. *Appl. Environ. Microbiol.* **76**, 922–926 (2010).

112. Pernthaler, A., Pernthaler, J. & Amann, R. Fluorescence in situ hybridization and catalyzed reporter deposition for the identification of marine bacteria. *Appl. Environ. Microbiol.* **68**, 3094–3101 (2002).

113. Teixeira, H., Sousa, A. L. & Azevedo, A. S. in *Fluorescence In-Situ Hybridization (FISH) for Microbial Cells: Methods and Concepts* (eds N. F. Azevedo & C. Almeida) 35–50 (Springer, 2021).

114. Hugenholtz, P., Tyson, G. W. & Blackall, L. L. in *Gene Probes: Principles and Protocols* (eds M. A. de Muro & Ralph Rapley) 29–42 (Humana Press, 2002).

Author contributions
P.B., B.G., T.B. and V.S. recorded MSI data. V.S., J.S., T.B. and K.D. assisted in the interpretation of results and writing the manuscript. T.B., V.S. and P.B. conducted the protocol validation experiments. P.B., B.G. and M.L. conceived and designed the study. P.B., B.G. and M.L. wrote the manuscript.

Competing interests
T.B. is an employee of Bruker Daltonics GmbH & Co. KG (Bremen). All other authors declare no competing interests.

Additional information
Supplementary information The online version contains supplementary material available at https://doi.org/10.1038/s41596-023-00864-1.

Correspondence and requests for materials should be addressed to Manuel Liebeke.

Peer review information *Nature Protocols* thanks Laura Sanchez and the other, anonymous, reviewer(s) for their contribution to the peer review of this work.

Reprints and permissions information is available at www.nature.com/reprints.

Related links
Key references using this protocol
Geier, B. et al. *Nat. Microbiol.* **5**, 498–510 (2020): https://doi.org/10.1038/s41564-019-0664-6
Geier, B. et al. *Proc. Natl Acad. Sci. USA* **118**, e2023773118 (2021): https://doi.org/10.1073/pnas.2023773118
Bien, T. et al. *Proc. Natl Acad. Sci. USA* **119**, e2114365119 (2022): https://doi.org/10.1073/pnas.2114365119
Niehaus, M. et al. *Nat. Methods* **16**, 925–931 (2019): https://doi.org/10.1038/s41592-019-0536-2